uc3m | Universidad Carlos III de Madrid

University Degree in Energy Engineering
Academic Year (2017-2018)

Bachelor Thesis

"Multi-criteria evaluation of power plants based on water use, thermodynamic and economic criteria"

Marina Olmeda Delgado

Tutor

Fontina Petrakopoulou-Robinson

Leganés, September 2018

Abstract

Electricity generation is an important sector for today's society and economy. With vast amounts of water spent in electricity production processes and water scarcity predicted to significantly rise in the near future, the necessity to evaluate water use in power plants arises.

Steam cooling processes in thermoelectric power plants are the main source of water use in electricity production. Even if other fluids, such as air, can be used for cooling purposes, water is associated with less costs and higher efficiencies.

This study evaluates the performance of two types of power plants: a natural gas combined cycle power plant and a integrated solar combined cycle power plant. Special focus is made on the cooling system used in the plants and its characteristics, such as water use, related costs and plant fuel requirements. Three different cooling systems are studied for each of the power plants: wet, dry and hybrid cooling. Wet cooling uses water as the cooling fluid and dry cooling uses air circulated by a fan to condense the steam. Hybrid cooling is a combination of the previous two methods based on the ambient conditions, considering the efficiency loss experienced by dry cooling systems in dry, warm weather.

To carry out this project the power plants are simulated using the software EbsilonProfessional and the plants are evaluated using exergy-based methods, i.e., exergetic, economic and exergoeconomic analyses. The results are used to compare the three different cooling options, as well as the water and fuel requirements of the different types of power plants.

Key words

Water conservation, natural gas, cooling system, combined cycle power plant, concentrating solar power, exergy, exergoeconomic analysis.

ACKNOWLEDGEMENTS

First of all, I wish to express my gratitude towards the tutor of this Bachelor Thesis, Fontina Petrakopoulou, for the help she has given me and for her availability and kindness every time I needed from her. This project would not have been possible without her.

Thanks to my friends, both the ones I have made in this university and the ones that have been with me for all my life, for having made my university years so enjoyable and unforgettable. Special mention to Miguel Ángel, my boyfriend, whom I met at UC3M and has given me his unconditional support in every aspect of my life, and Alejandra, who has studied with me every single exam since my first university year.

Above all, I want to thank my parents and my brother for having taught me everything I need to know. Without the economical and emotional support from my parents, I would not have been able to finish my studies. Thanks to them I have learnt English, travelled the world, and grown up with a clear determination to study hard and get a university degree.

INDEX

FIGURE INDEX

TABLE INDEX

NOMENCLATURE

Abbreviations

NGCC	*Natural gas combined cycle*
CSP	*Concentrated solar power*
GT	*Gas turbine*
ST	*Steam turbine*
HRSG	*Heat recovery steam generator*
HP	*High pressure*
IP	*Intermediate pressure*
LP	*Low pressure*
SH	*Superheater*
EVAP	*Evaporator*
ECON	*Economizer*
RH	*Reheater*
COMP	*Compressor*
CC	*Combustion chamber*
G	*Generator*
COND	*Condenser*
AC COND	*Air-cooled condenser*
DNI	*Direct normal irradiance*
FCI	*Fixed capital investment*
PEC	*Purchase equipment cost*
O&M	*Operating and maintenance*
TRR	*Total rate of return*
COE	*Cost of electricity*

Symbols

E	*Exergy*
$\dot{E}$	*Exergy rate*
c	*Cost per exergy unit*
$\dot{C}$	*Cost rate of exergy stream/component*
T	*Temperature*
p	*Pressure*
$\dot{m}$	*Mass flow rate*
ε	*Exergetic efficiency*
y	*Exergy destruction ratio*
$\dot{Z}$	*Investment cost rate*
f	*Exergoeconomic factor*
r	*Relative cost difference*

Subscripts

k	$Component\ index$
D	$Destrustion\ (exergy)$
F	$Fuel\ (exergy)$
P	$Product\ (exergy)$
CH	$Chemical\ (exergy)$
PH	$Physical\ (exergy)$
TOT	$Total$

1. INTRODUCTION

1.1. Motivation

Water accessibility is necessary to ensure economic development. People living in poverty circumstances have trouble to get access to drinking water, experiencing problems also with personal hygiene and sanitation. This results in a lot of health issues, most of them related to consuming non-drinkable water, which can cause up to 2.18 million deaths annually, most of them of children under 5 years old [1]. Furthermore, agriculture and animal breeding are associated with the highest water expenditure among all activities, so water scarcity creates a food shortage problem and the consumption of food of bad condition (animals can carry illness due to the consumption of dirty water, while vegetables watered with dirty water can cause health issues) [2]. Water scarcity does not necessarily imply physical water scarcity, but it can be related to factors like politics, policies and socioeconomic relations (social water scarcity) [3]. In addition to the sectors mentioned, water plays a very important role in energy generation.

The use of water is a crucial element in the production of electric power in all different kinds of power plants, particularly in thermoelectric generation, i.e., fossil fuels, nuclear, solar thermal, geothermal. In thermoelectric power plants steam is obtained by heating water with a specific energy source (fossil fuel, solar energy, nuclear fission, heat from underground water reservoirs). That steam is used to make power plant turbines spin and generate electricity. After the steam is used, there is a necessity to condense it and convert it to water. To realize the condensation of the steam large amounts of a cooling agent are required. This cooling agent is in most cases water [4].

The high reliability of the energy sector on water availability and the more and more frequent water shortages globally, reveals the importance of the study of water use in power plants.

1.2. Aim of the study

This study aims to give visibility to water use in electricity production, as well as to propose different alternative cooling systems with which water use in thermal power plants can be reduced significantly. The power plants presented and evaluated are natural gas and hybrid solar-natural gas plants.

The steps followed in order to realize this Bachelor Thesis were the following:

- Literature survey on the use of water in electricity production and steam cooling methods.
- The simulation of a natural gas combined cycle (NGCC) and a concentrated solar power (CSP) integrated combined cycle power plant using the software EbsilonProfessional.
- Operational modifications of the plants using three different cooling systems: wet recirculating cooling, dry-cooled and hybrid cooling.

- Realization of exergetic and exergoeconomic analyses of the power plants and the different cooling methods using MATLAB.
- Realization of a detailed economic analysis of the power plants.
- Sensitivity analyses of the variation of the cost of electricity with the costs of water and fuel.
- The comparison between the NGCC and CSP integrated combined cycle plants based on water requirements, costs and fuel needs has also been realized.

2. LITERATURE SURVEY

In order to understand the water use in the electricity production process the difference between withdrawal and consumption has to be established [5]. Withdrawal refers to the amount of water that a power plant takes from a water source (river, lake, ocean, underground reservoirs, etc). Within the amount of water withdrawn, some of it will be poured again into the given source where it was taken from, and some of it will be evaporated in the cooling process or incorporated into by products and will not make it back. That amount of water that is lost through the process is called consumption [6].

With thermoelectric power plants having a total withdrawal share even higher than that of agriculture in countries such as the United States (US) [7], the energy-water nexus has become an important topic within the world energy production. The main factors influencing this water dependence of energy can be classified in three categories: geography and climate, technology used and location and community [8]. A problem arises in areas with scarce water resources, like the north part of China, where the water available is not enough to meet all power needs, especially considering the big amount of coal reservoirs in that same part of the country. [9] In addition to this, it is necessary to take into account the fact that energy demand is going to continue in a rising tendency as economy also grows, and that some years from now water shortage will be even more severe, affecting more than half of the world's population. This is due to the effect of climate change in temperatures, precipitations and rising sea level, which will result in the contamination of freshwater sources [10][11].

Even though some power plants might use the same cooling technology, the water consumption varies depending on the energy source. If we establish a comparison between natural gas and coal power plants, for example, it can be observed that natural gas power plants use less volume of water per unit of electricity produced. This is due to lignite extraction being more water-consuming than that of natural gas, as mines have to be dewatered. Also, the higher efficiency of natural gas when compared to coal must be considered, given that less energy is required to get electricity out of it. This has lead people to think that a possible solution to save water from energy production might be using natural gas instead of coal in the already existing power plants, but that would as well imply the necessity of changing power plants technologies, which is time-consuming and expensive [12].

2.1. Cooling technologies in power plants

Among the most commonly used cooling technologies in thermoelectric power plants are: once-through cooling, recirculating wet cooling, dry cooling and hybrid cooling.

2.1.1. Once-through cooling

This open loop system takes a vast amount of water from a close source and circulates through some pipes to be used in the steam cooling process. After the water is used, most of it is poured back into the source it was taken from. This method requires power plants to be located near large natural water reservoirs, which limits siting options and makes power plants using this method very sensitive to drought [13]. Even though the water consumption is very low, it has a big environmental impact due to the large amounts of water withdrawn (around 20,000-60,000 gallons per MWh of electricity produced), the intake structures and the big amounts of warmer water discharged, which can raise considerably the average temperature of the mentioned body of water, causing important damage to the aquatic species [14]. This cooling method is now only used in older power plants, having been replaced by recirculating wet cooling due to environmental restrictions.

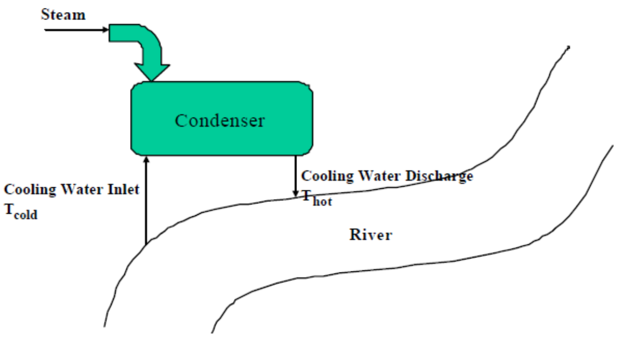

Figure 1. Once-through cooling scheme [15]

2.1.2. Recirculating wet cooling

In contrast to the previous cooling method, recirculating wet cooling involves a closed loop system, with the water flowing from the condenser of the plant to a cooling tower. Part of the cooling water is evaporated, some of it is recirculated and reused in the next cooling cycle and a small part is discharged back to the water source. The cooling water is first used to condense the steam exiting the steam turbine of the power plant, then it is brought into contact with ambient air to drop its temperature back to its initial one, and it is then sent back to the condenser. As there are some evaporation losses, there is a need of makeup water in the cooling tower, that is about 2-3% of the total recirculating water and is the main cause of withdrawals in wet cooling. When compared to once-through systems, recirculating systems consume a relatively higher part of the water withdrawn, mostly due to high evaporation losses (around 75%). Despite the higher consumption, this method requires a much lower amount of water withdrawn from the water source and avoids high temperature water discharges, causing less damage to the aquatic species, which is why it is used instead of once-through cooling since the 1970s. Reported capital costs of this technology are around 60-80 €/kW [16].

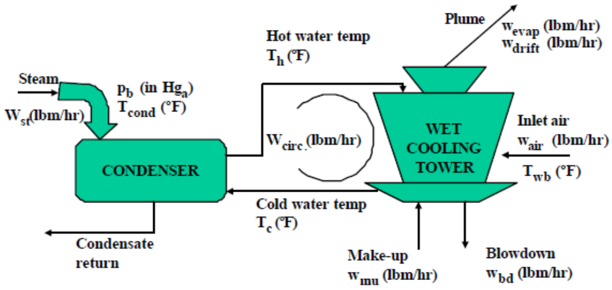

Figure 2. Recirculating wet cooling scheme [15]

2.1.3. Dry cooling

It works similarly to the recirculating system, but its main characteristic is the use of air instead of water as a cooling fluid. In this way both withdrawal and consumption of water are avoided, but imposes higher costs (infrastructural investment; electricity to power fans; capital costs around 150€/kW; and a cost of electricity around 3€/MWh higher than that of wet cooling [16]) and lower efficiencies, requiring more fuel per electricity unit. The higher mass flow of fuel required is due to the power input needed to work the air-cooled condenser fan. These lower efficiencies imply a loss of output of 2-3% per year on average but can get to a 20-30% when demand is at its peak, usually in summer, when its efficiency is lowered due to hot and dry weather. The fact that the efficiency is lower in dry weather is highly inconvenient given that it is the kind of weather where dry cooling is more necessary [17]. It works using heat exchangers: water flows through the heat exchanger tubes while air goes through it. Its use might be especially suitable for solar thermal power plants, that show a higher efficiency in places with high direct normal irradiation, which usually means water scarcity and higher temperatures, but the low efficiency of the cooling system at high temperatures can be balanced by the high efficiency of the concentrators in such conditions [18].

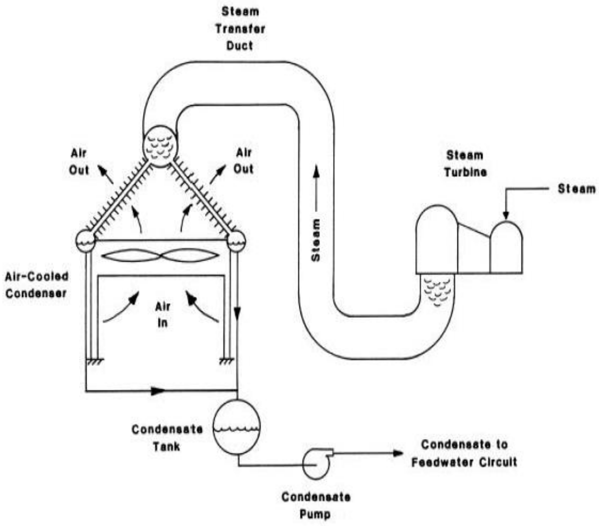

Figure 3. Dry cooling scheme [15]

2.1.4. Hybrid cooling

Hybrid cooling is considered a closed loop system which uses a combination of air-cooled condensers, condensers and cooling towers either operating together or in separate ways to decrease the water use. This cooling method can eliminate up to 80% of the water used. It consists of a wet and a dry section: the wet section includes a cooling tower while the dry section consists of an air-cooled condenser. Both sections can be in parallel or series [19].

- Parallel hybrid cooling: Steam coming from the turbine is cooled by the cooling water. After that, part of that water, now warmer, goes to the cooling tower directly, and the other part is diverted through the dry cooling system, lowering its temperature and entering the cooling tower's pond where it mixes with the rest of the cooling water and makeup water. The water coming out of the cooling tower, now cold, cools the steam coming from the turbine again. Another option is splitting the total mass flow of steam into two parallel flows: one going through dry cooling and the other one going through wet cooling.
- Series hybrid cooling: In this system, once the cooling water has a higher temperature after cooling the steam, it is directed to the cooling tower, but again part of it is diverted through a dry cooling system. The difference in this case is that dry cooled water is then mixed with the hot one before entering the cooling tower, making the overall temperature of the water to be cooled lower [20].

2.2. Environmental and economic issues of water use in power plants

There is a high risk to aquatic species living in freshwater sources that are used for cooling purposes. Intake structures for water withdrawals are an example of a threat to biodiversity, causing species death when accidentally going through them. Also, the withdrawal itself means that a lot of water is taken from its original place, disrupting water sources natural course and structure and highly affecting flora and fauna. One of the main concerns, though, is the high temperature of the effluents that are poured back into the source where they were withdrawn from in once-through cooling systems, where these are especially abundant. The temperature rise of these effluents varies from 8 to 15ºC more than the temperature of the water initially withdrawn. This rise in water temperature affects in different ways each of the species, as some are able to stand higher temperatures than others due to a higher critical thermal maximum. The critical thermal maximum is the temperature above which species are not able to survive for an extended time [21]. Some of the drawbacks of higher temperatures in natural water sources include decreased oxygen solubility and increased respiration rates, which implies reduced oxygen in water. A higher temperature in water may as well reduce biological processes (including growth) a 10% per 1ºC increase, and make chemicals toxicity and species vulnerability to those increase [14]. The fact that depending on the location of the power plant there is existence of different organism and fishes, each of them having a different critical thermal maximum, makes it difficult to establish a higher bound to the temperature of effluents discharged from a power plant. There has been US states, though, that have set a maximum water surface temperature of 32ºC, while the European Union has established that temperatures downstream from discharge point should not be above 21.5ºC for salmonid waters, and 28ºC for cyprinid waters [22].

Furthermore, water saving methods in thermoelectric power plants would mean not only an environmental advantage and a way to sort out the issue of electric power generation in locations with water scarcity. It would also be an economic measure, allowing power plants to depend less on nearby water sources in a way that they can supply electricity in a more continuous way even in times of drought. There is also a marginal of the gallons of water that would not be withdrawn if water saving retrofits where applied to cooling systems. However, cooling systems using water are nowadays the most cost-effective ones, so the answer to the economic problem of water use in electricity production would not be as simple as using dry cooling [23].

On the other hand, the energy-water nexus plays an important role in the economic growth of a nation, as it implies higher demand of energy (which implies, at the same time, water) and water for personal consume by the population [24].

Table 1. Comparison of cooling technologies [15]

Cooling technology	Consumption	Withdrawal	Costs	Environmental impact
Once-through cooling	Low consumption compared to withdrawal	20,000-60,000 gal/MWh	Lowest installation and operational costs of all cooling technologies	High temperature water discharges and big amounts of water withdrawn, causing damage to aquatic species
Wet recirculating cooling	400-1,000 gal/MWh	500-1,200 gal/MWh	Higher costs than once-through cooling technologies (operating costs around 4-10 €/kW)	More water consumed than in any other cooling technology
Dry cooling	Negligible	Negligible	Highest installation and operational costs (around 80-200 €/kW) of all cooling technologies	No significant environmental impact due to dry cooling
Hybrid cooling	30-80% less than wet cooling	Variable depending on air and water percentages	Variable	Variable depending on air and water amounts used

2.3. Water use in thermoelectric power plants

As it has already been mentioned, cooling technologies are the main responsible for water withdrawal and consumption in power plants. However, there are also some secondary water losses that may vary from one type of power plant to another.

2.3.1. Solar thermal power plants

Solar thermal power plants perform better thermodynamically in climates with high solar radiation. The main issue with this is that those climates very often happen to experience water scarcity, with little amount of water sources available. It would make sense then, to use dry cooling in this type of power plants, but it also has been mentioned that dry cooling presents lower efficiency in dry climates, so it would be necessary to analyse this possibility [25]. Apart from cooling, solar thermal power plants use water with other purposes which include: boiler make-up water; eliminating dust during plant construction; water for disassembling; operational requirements; and cleaning of mirrors (around 0.08-0.15 m^3/MWh), which has to be done even more often to avoid efficiency losses in locations with dry weather and presence of dust [26].

2.3.2. Coal power plants

Besides the water destined for cooling, coal power plants use a smaller, but still relevant, amount of water for coal extraction (around 617,000 gal of water per ton of coal) and transportation (9,000 gal of water per ton of coal transported). Also there are some water losses related to coal cleaning (around 17,000 gal/MWh [27]), boiler make-up water, ash handling and flue gas desulfurization [28] [29]. Reported water footprint of coal power plants is around 0.16 m^3/GJ [8].

2.3.3. Natural gas power plants

Natural gas power plants water use that is not related to cooling processes include: fuel extraction, with water use in the case of shale gas extraction (hydraulic fracturing) ranging from 300,000 to 9,000,000 gallons per well, higher than that of natural gas; and processing to get pipeline quality (4-5 gal/MWh in natural gas and 16-17 gal/MWh in shale gas) [27][30]. Natural gas water demand is 0.025 m^3/MWh [8].

2.3.4. Oil power plants

Water demand for oil oscillates between 0.1008 and 0.2592 m^3/MWh. This can be divided into production (conventional crude oil production, oil sands production and oil shale production) and refining [8].

2.3.5. Nuclear power plants

Nuclear power plants use water for mining and processing (milling, conversion, enrichment, fuel fabrication and reprocessing) [30], and they have the particularity of being the type of power plants that uses more water quantity, as cooling requires more of it. This is because steam operates at lower temperatures and pressures, which results in lower efficiencies, so the quantity of steam must be higher. This translates in bigger amounts of cooling water to produce a certain amount of electricity compared to other thermoelectric power plants [31].

2.4. Water use in other types of power plants

Although most of the water used in the electricity production sector has cooling purposes, there is also a big water footprint in those power plants that use a non-thermoelectric technology (hydroelectric, wind, solar photovoltaic).

2.4.1. Hydroelectric power plants

Even though hydroelectric power generation rely entirely on the water source where the dam is built, little amount of water consumption is observed when using this source, being most of it due to evaporation and seepage in reservoirs surface. There is a problem for the aquatic environment though, given that the construction of a dam alters highly the habitat of many species, causing the destruction of flora and fauna [32].

2.4.2. Wind power plants

Wind power uses negligible amounts of water compared to other sources, being that use limited to cleaning purposes. Wind power plants, though, rely on other thermoelectric power plants (fossil fuels, nuclear) in moments when wind is no sufficient to generate enough electric power [33].

2.4.3. Solar photovoltaic plants

Although nowadays water in solar photovoltaic power plants does not have an important role, limited to cleaning panels, there is some research being made about increasing the panels efficiency by using cooling systems. This relation is done due to the panel efficiency loss when it reaches high temperatures. Using a cooling fluid (water, air, hybrid) would improve the efficiency of the panel and at the same time, the heat extracted could be used as thermal power, combining in this way solar thermal and photovoltaic power. This area, though, is still going through research [34].

3. PLANT DESCRIPTION

This study starts with the simulation of a NGCC power plant and a CSP integrated combined cycle power plant in EbsilonProfessional. For each power plant there are three simulations, each of them with a different cooling system: wet recirculating, dry and hybrid cooling. To correctly analyse the performance of each of them, three analyses are carried out: exergetic, economic and exergoeconomic analyses.

3.1. Simulation of the NGCC

A combined cycle uses both a gas turbine (Brayton cycle) and a steam turbine (Rankine cycle) to produce electricity, increasing in this way the power output and efficiency compared to a single power generation cycle.

A gas turbine (GT) cycle is composed of compressor, combustion chamber and expander. Air enters the compressor at ambient conditions and is compressed and led to the combustion chamber. Fuel is injected to the combustion chamber to realize the combustion once in contact with air. High temperature flue gas coming from the combustion chamber goes to the turbine or expander and make it spin getting a power output from it. A steam turbine (ST) cycle boils water to produce steam to make the steam turbine spin and get in this way a power output. This steam is later condensed back to liquid water and compressed by means of a pump to go through the boiler again and form a closed cycle. In a combined cycle power plant, a heat recovery steam generator (HRSG) uses the exhaust gases from the gas turbine cycle to produce steam for the steam turbine cycle, substituting in this way the boiler and getting extra power from it. This exhaust gases would otherwise be discarded in a simple GT cycle [35].

The NGCC simulated here uses natural gas, assumed to be 100% CH_4, and has a three-pressure level steam turbine with a reheating stage between the high pressure (HP) and intermediate pressure (IP). The plant has a power output of 427 MW kept constant throughout the study. The thermal energy after the gas turbine is transferred to water in a three-pressure level HRSG and further used in the steam turbine. In this simulation, the gas turbine and steam turbine power outputs are 285 MW and 143 MW, respectively and the efficiency of the combined cycle is 58.2 % when using a wet cooling system (base case). The simulation ambient temperature is 15°C, assuming this will change throughout the year.

The heavy-duty gas turbine of Siemens SGT5-4000F (50 Hz) is used as a model to simulate the gas turbine. To accurately simulate the gas turbine in the simulation software EbsilonProfessional, specific variables are considered. The objective here is to achieve the design of a gas turbine as similar as possible to the real one, using various operational parameters and minimizing the difference between the real gas turbine and the one designed for this project.

The gas turbine library in Ebsilon provides the data of the gas turbine SGT5-4000F model. The simulation assumes three separate components for the design of the gas turbine: a compressor, a combustion chamber and an expander. Parameters like power output, efficiency, inlet and exhaust temperature and fuel mass flow are compared, obtaining the results shown in Table 1.

Table 2. Comparison between theoretical and simulated gas turbine

Parameter	Data for SGT5-4000F from Ebsilon gas turbine library	Actual value in simulation	Error (%)
Power output (kW)	285,000	285,017	6.3×10^{-3}
Exhaust mass flow (kg/s)	685	693.7	1.27
Exhaust temperature (°C)	580	582.9	0.5
Inlet temperature (°C)	15	15	-
Inlet pressure (bar)	1.013	1.013	-
Fuel inlet mass flow (kg/s)	14.653	14.66	0.05
Air inlet mass flow (kg/s)	676.585	679.09	0.37
Gas turbine efficiency (%)	38.92	38.87	0.13

Given the small errors calculated, the gas turbine modelled in the simulation is considered equivalent to SGT5-4000F.

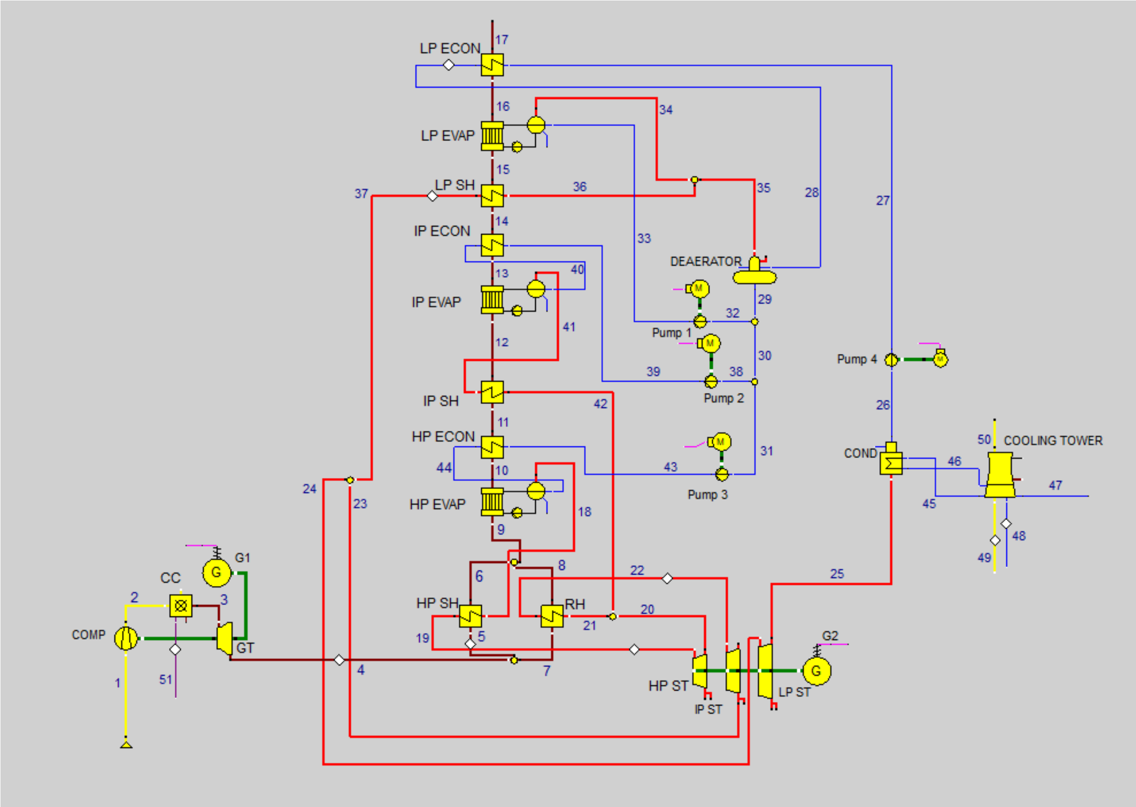

Figure 4. NGCC power plant with wet cooling system

Air enters the compressor (stream 1) and, after its pressure is increased, it is led to the combustion chamber. Natural gas is injected to the combustion chamber with a mass flow of 14.66 kg/s (stream 51) to realize the combustion, achieving the maximum temperature of the whole cycle at the outlet of the component (stream 3 with 1239.86 °C). The combustion products with 693.66 kg/s and a pressure of 1.058 bar pass through the expander of the gas turbine system to then enter the HRSG of the plant. The HRSG generates steam for the steam turbine comprised of three pressure levels, each of them counting with a superheater, an evaporator and an economizer. High-pressure steam at 563°C and 125 bars (stream 19) is expanded to 25 bars (stream 20), to then go through the HRSG again to be reheated back to 563°C (stream 22). Reheated steam returns back to the steam turbine at the intermediate pressure (IP) level, and it is expanded to 5 bars (stream 23). Low-pressure steam is expanded from 5 bar (stream 24) to 0.05 bar (stream 25) in the low-pressure steam turbine (LP ST). The maximum pressure of the cycle is 137.06 bar at the inlet of the high-pressure economizer (HP ECON) (stream 43). The simulation reaches its minimum pressure in stream 25 coming out of the steam turbine. The generated steam is then condensed into liquid water to enter the LP ECON to increase its temperature, so it can go through the deaerator and this way form a closed cycle. To realize that, steam has to go through the cooling system, which is different for each simulation. Three power plants with the same characteristics are simulated only varying the cooling system among them. The water from condensing the steam then goes through a pump to increase its pressure and send it to the HRSG to be used again.

3.1.1. The NGCC power plant using wet cooling

This simulation includes the already described NGCC and uses wet cooling as a cooling system.

The wet cooling system consists of a closed system composed of a condenser and a cooling tower. Steam with a mass flow of 103.59 kg/s (stream 25) goes through the condenser and it is condensed by means of cooling water at a rate of 9736.49 kg/s (stream 45). Cooling water exits the cooling tower, goes through the condenser and goes back to the cooling tower. There, this higher temperature water comes into contact with ambient air at a rate of 4868.20 kg/s (stream 49) to decrease the temperature of the cooling water, so that it can be reused. Some part of the water is evaporated in the process and, therefore, lost, so there is a stream of make-up water going into the cooling tower with a mass flow of 102.82 kg/s (stream 48).

3.1.2. The NGCC power plant using dry cooling

The simulation using dry cooling only differs from the one already described in the cooling system, which alters slightly the characteristics of some streams.

For the dry cooling system, an air-cooled condenser is used. In this case steam is condensed using air as the cooling fluid circulated with a fan. A mass flow of air of 302073.16 kg/s (stream 45) is used to condense 105.34 kg/s of steam (stream 25). No water is used in this cooling system, but there is an efficiency loss due to the power input of 7.2 MW to work the fan, which also implies a rise in costs. This efficiency loss is even higher during warm months. Due to this power input needed for the fan, the fuel mass flow needed is slightly higher than the one already mentioned for the power plant using wet cooling: 14.91 kg/s (stream 47). This has also an effect on the combustion products mass flow, that this time is of 705.46 kg/s (stream 3).

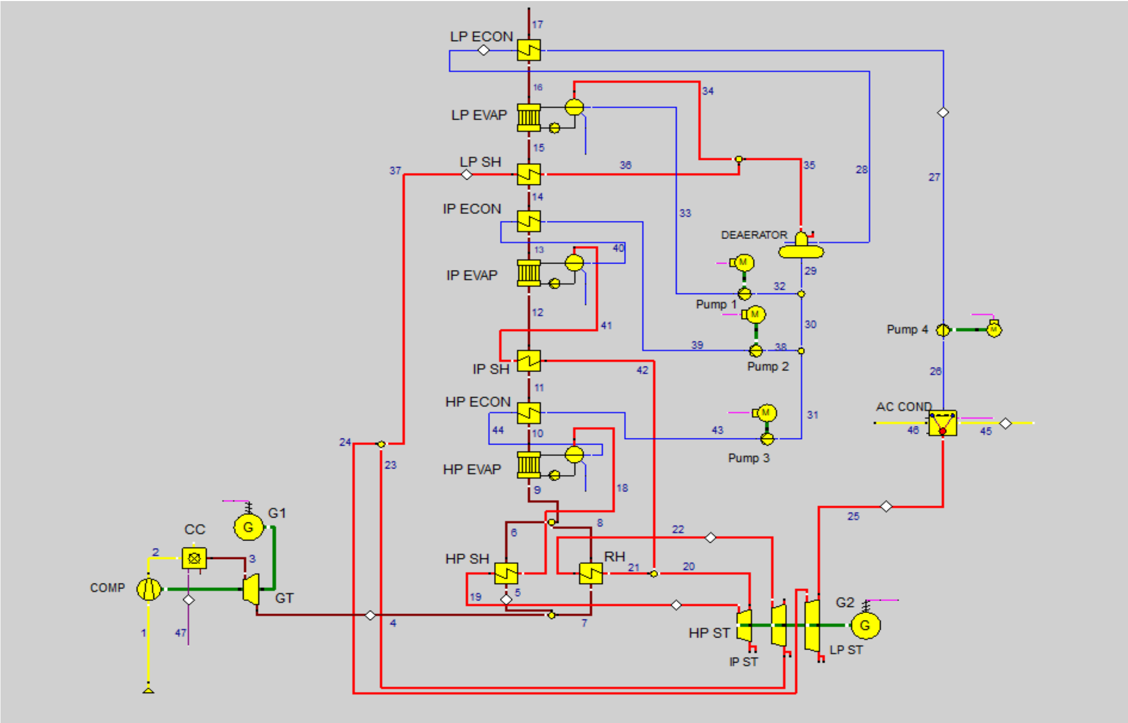

Figure 5. NGCC power plant with dry cooling system

3.1.3. The NGCC power plant using hybrid cooling

The hybrid cooling system splits the mass flow of steam coming out of the steam turbine into two parallel flows: one goes through wet cooling, and the other stream goes through an air-cooled condenser (dry cooling), so any distribution of the total mass flow of steam can be chosen to go through wet and dry cooling. In this study, two design cases are considered. Due to the mentioned efficiency loss of the air-cooled condenser during warm and dry months, the power plant uses wet cooling during these months of the year, with no mass flow of steam going through dry cooling to be condensed. Alternatively, all the mass flow of steam coming out of the steam turbine goes through the dry cooling system during colder months. For simplicity reasons the hybrid cooling system is considered to work in dry cooling mode and wet cooling mode both for six months a year.

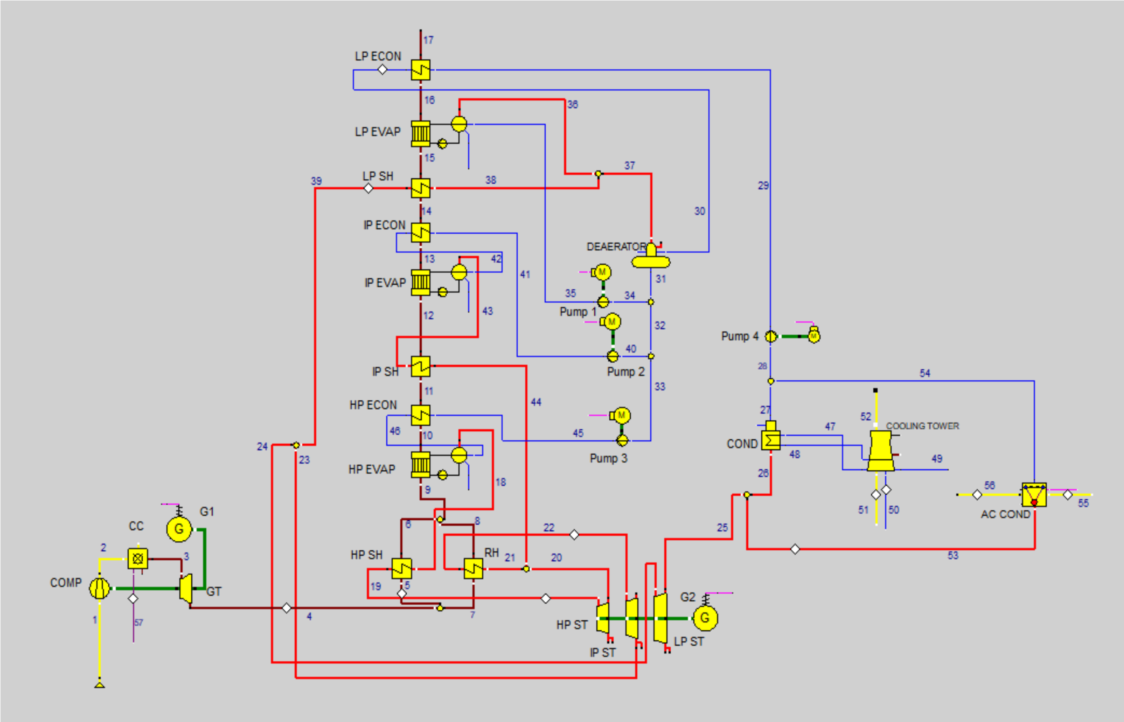

Figure 6. NGCC power plant with hybrid cooling system

3.2. Simulation of the CSP integrated combined cycle

The integrated solar combined cycle simulation is composed of a concentrated solar power (CSP) field and a natural gas combined cycle. This combination of technologies presents advantages such as the reduction of fossil fuel consumption (lower mass flow entering the combustion chamber needed) and reduction of CSP costs compared to a single CSP power plant. However, it implies a considerably high rise in investment costs when compared to a simple combined cycle [36].

CSP technology is characterized by the use of mirrors or lenses to concentrate the sun rays to heat a thermal fluid that is used for the production of steam [37]. This steam usually spins a steam turbine and a power output is obtained in this way. Two types of CSP technologies can be found: line-focusing systems, when the irradiance is concentrated along a line (parabolic trough, linear Fresnel); and point-focusing systems, concentrating the irradiation on a single focal point (solar tower, solar dish) [38].

The concept of integrated solar combined cycle uses the CSP heat either to produce additional steam for the steam turbine, that is integrated in the HRSG of the combined cycle, for what line focusing systems are ideal (parabolic trough or linear Fresnel); or to heat the compressed air before entering the combustion chamber [36].

In the simulated power plant, the CSP technology used is parabolic trough. Parabolic trough technology consists of long arrays of mirrors (solar collectors) with parabolic shape that concentrates the solar irradiance to heat a pipe containing thermal fluid [39]. This thermal fluid in the case of the power plant of the study is led to a HRSG to generate additional steam to integrate to the steam turbine of a combined cycle power plant through the 3-pressure level HRSG and, in this way, reduce the fuel mass flow necessary to get the desired power output. The parabolic trough solar field consists of 7500 collectors of 10 m length located in Sevilla (37.39° north, 5.96° west).

In order to consider every possible working condition for the CSP power plant, both a design and an off-design model have been simulated, so that later real data over time can be applied to the off-design model to get a dynamic simulation.

In the design simulation, the date and time chosen for the ambient conditions is the 21st of June (summer solstice) of 2017 at 12:00. The direct normal irradiance (DNI) is assumed to be 950 W/m^2, and the ambient temperature is 33.4°C. The ambient temperature is obtained by taking real hourly ambient temperatures in Sevilla during the years 2005-2009 (both included) and getting a mean temperature for each hour for a whole year. This mean hourly temperatures will be used as an input for the off-design dynamic simulations.

In this case the gas turbine model used is SGT5-4000F. It is the same gas turbine model as the one chosen for the NGCC simulation, but this time, as the power output is set to 427 MW, the fuel mass flow is variable depending on the date and time and how much power is achieved from the sun. When adding a CSP field to the combined cycle, the amount of natural gas injected to the combustion chamber is lower during those hours of the day when there is sun activity. During night hours, or even cloudy days, the power plant works as a normal combined cycle.

The solar field is connected to a two pressure levels HRSG (HRSG 1), using a three-pin controller to determine the mass flow (corrected value) of oil running through the field from the value of the enthalpy. There is a pump to compress the oil at the inlet of the solar field.

The steam produced in the HRSG 1 is integrated in the HRSG of the combined cycle (HRSG 2) with three pressure levels (high, intermediate and low) to increase the steam production. To do this, liquid water inlet streams of the HRSG 1 HP and IP economizers are an extraction from the inlet streams of the HRSG 2 HP and IP economizers. At the same time, the HRSG 1 HP and IP superheaters outlet steam streams are injected to the outlet of the HP and IP HRSG 2 evaporators, increasing in this way the steam production. This will make the power output of the 3-pressure level steam turbine higher, which will allow a lower mass flow of fuel entering the combustion chamber and a higher combined cycle efficiency.

Again, three different simulations have been made of this power plant model, each of them using a different cooling system: wet, dry and hybrid cooling. The differences between each of them resides only in the refrigeration system used. The hybrid cooling power plant is going to work either fully dry or fully wet cooling at a time, depending on the time of the year considered, so the results obtained in both wet and dry cooling simulations can be applied to the hybrid cooling power plant as well.

To calculate the total electric power output of the CSP parabolic trough technology in the static simulation conditions, an identical power plant has been simulated, only lacking the

CSP technology, so it is possible to see the contribution of the solar field to the electrical power obtained from the steam turbine. In such power plant we observe a ST power output of 145 MWe, while the reported ST electric power output adding CSP technology is 224 MWe. This makes the electric power output of the CSP power plant integrated of 79 MWe. Considering that the CSP technology counts with an effective heat of 258 MW, this would make the capacity factor of the power plant of 30.65% for the design date and time.

3.2.1. The CSP integrated combined cycle power plant using wet cooling

Two different parts are observed in this simulation: the CSP power plant and the NGCC power plant. The CSP power plant consists of a parabolic trough solar field composed of 7500 collectors. During daytime, whenever there are no clouds, the direct normal irradiance from the sun hits the collectors' surface and generates a heat that is used to heat thermal oil with a mass flow of 1047.71 kg/s in the design simulation. This oil, once heated from 294.31°C (stream 22) to 395°C (stream 14), is led to a two-pressure level HRSG (HRSG 1), with superheater, evaporator and economizer in each pressure level. HRSG 1 extracts liquid water from the combined cycle three-pressure level HRSG (HRSG 2) and heats it to produce steam. The steam produced is injected back in HRSG 2. After passing through the HRSG 1, the thermal oil, now at a lower temperature of 293.32°C (stream 21), needs to be compressed from 35 to 50 bar by means of a pump, so that it can be heated again by the solar field (stream 22).

In the combined cycle part, the air at ambient conditions (stream 1) is compressed to 15 bars (stream 2) by the compressor and is then led to the combustion chamber. The fuel mass flow injected in the combustion chamber is variable in this type of power plant. However, considering in this case the static simulation with DNI of 950 W/m^2 and ambient temperature of 33.4°C, the mass flow of natural gas needed to meet the power output requirements (426.92 MW) is 11.365 kg/s (stream 72) for wet cooling. The cycle reaches its maximum temperature at the outlet of the combustion chamber, with 1231.88°C (stream 3). Combustion products at 544.75 kg/s pass through the gas turbine, and then enter the HRSG 2, with three pressure levels, that generates the steam for the steam turbine. HRSG 2 high and intermediate pressure levels are composed of superheater, evaporator and economizer, while the low-pressure level is formed by evaporator, economizer and preheater. High-pressure steam at 532.00°C (stream 34) is expanded from 129.65 to 39.75 bar (stream 35) and is then mixed with intermediate-pressure steam coming from the HRSG 2 at 320.68°C and 39.75 bar (stream 59), to be expanded to 4.8 bar (stream 37). This steam is again mixed with the low-pressure steam at 151.84°C and 5 bar (stream 50) and is expanded to 0.05 bar (stream 40). Highest pressure of the whole cycle is found at the inlet of the high-pressure economizer of both HRSG (both the one of the CSP plant and the combined cycle), which is 130 bars (streams 61, 62 and 27). Lowest pressure of the cycle is found right after the steam turbine (stream 40): 0.05 bar (for the static simulation). Steam coming out of the steam turbine is then condensed into liquid water to enter the preheater. To realize that, steam passes through the cooling system, which in this simulation consists of a condenser and a cooling tower.

The mass flow of steam to be condensed is 189.79 kg/s and has a pressure of 0.05 bar (stream 40). Cooling water coming from the cooling tower at a rate of 16207.28 kg/s (stream 66), goes through the condenser and is then led back to the cooling tower (stream 67), where an air mass flow of 8103.56 kg/s (stream 70) cools down these higher temperature water in order to be used again as cooling water. Evaporation losses are compensated by a make-up water stream of 140.04 kg/s (stream 69). After steam is condensed it is led to the preheater (stream 42), where liquid water temperature is increased, so it can go through the deaerator and form a closed cycle.

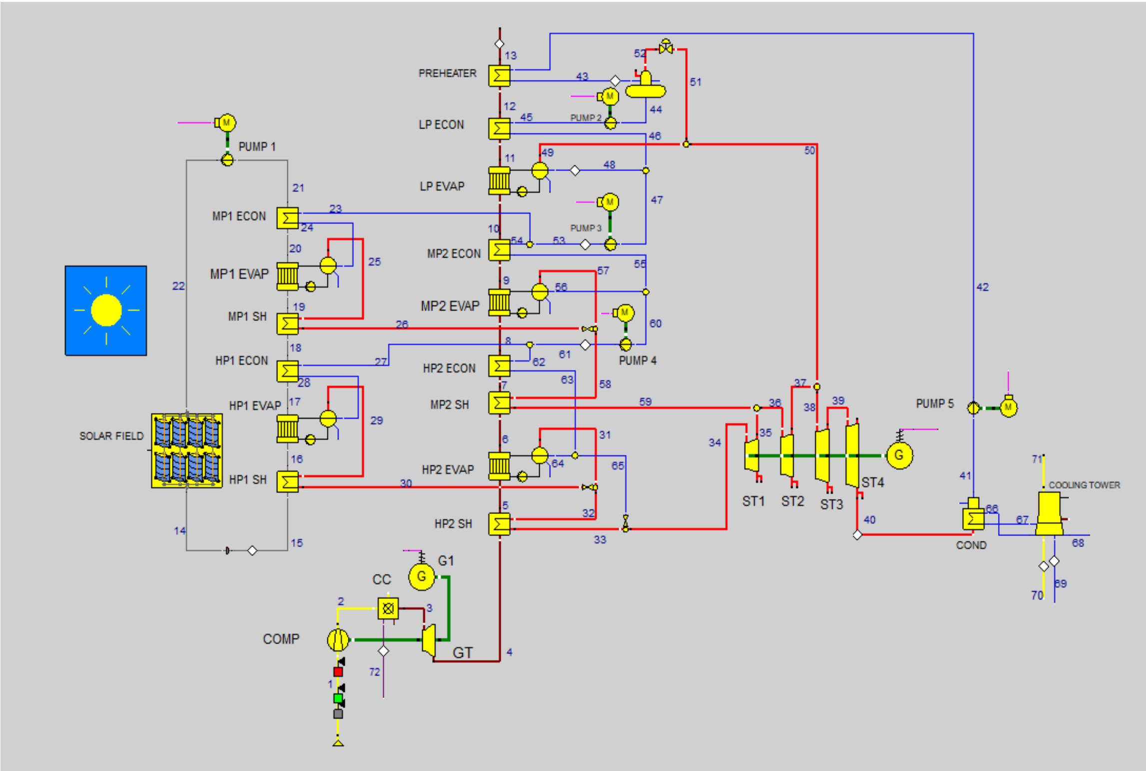

Figure 7. CSP integrated combined cycle with wet cooling system

3.2.2. The CSP integrated combined cycle power plant using dry cooling

The simulation using a dry cooling system has the same characteristics as the one previously described but including some differences. The cooling system consists of an air-cooled condenser that needs a power input to work the fan that circulates the air to condense the steam. This power input makes the mass flow of fuel (stream 68) needed to meet the power requirements (427 MW) be higher, with 12.22 kg/s for the static simulation. Because of this rise in fuel consumption, combustion products have a mass flow of 585.91 kg/s and a temperature of 1251.71°C this time (stream 3).

The next difference found in this simulation is the pressure of the steam coming out of the steam turbine, that is 0.12 bar (stream 40). This is due to the high temperature of the air (33.4°C) in the air-cooled condenser, which leads to a higher steam pressure so that it can be condensed easier with less efficiency losses. The temperature of the air is that of the environment.

Regarding the cooling system, steam with mass flow of 195 kg/s (stream 40) is condensed by air at a rate of 41567.61 kg/s (stream 66) circulated by a fan. The power input to work the fan is 10.5 MW, this time higher than it was in the NGCC power plant mainly due to the higher mass flow of steam to be condensed, as there is additional steam provided by the solar field.

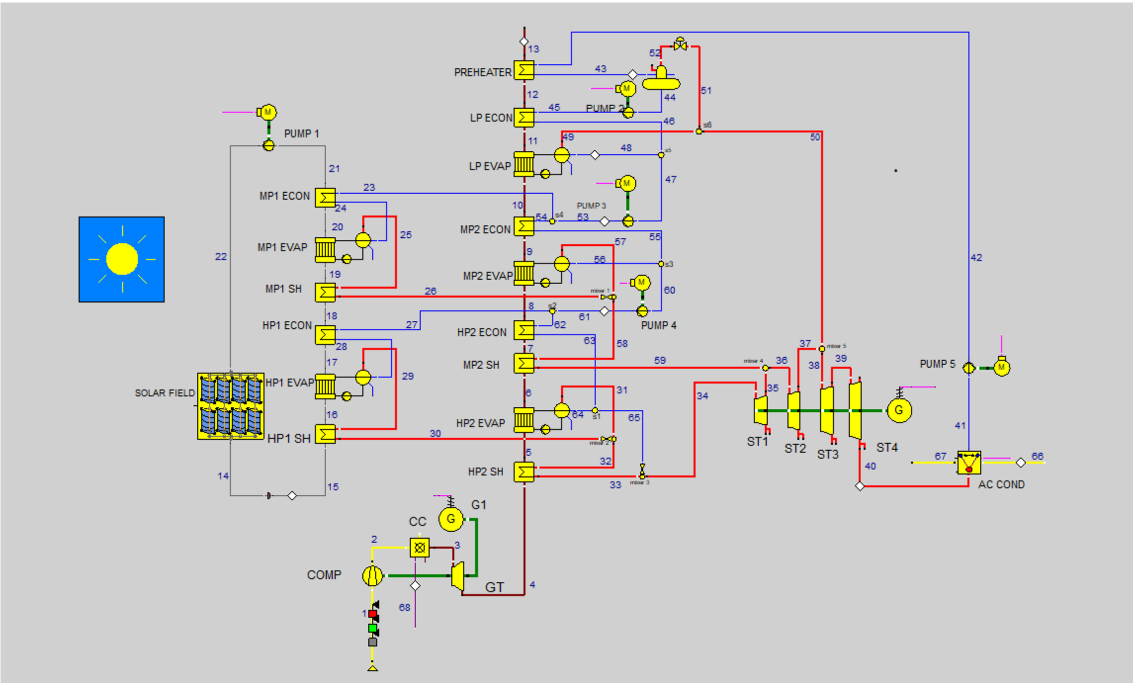

Figure 8. CSP integrated combined cycle power plant with dry cooling system

3.2.3. The CSP integrated combined cycle power plant using hybrid cooling

The power plant including a hybrid cooling system includes both a wet cooling system and an air-cooled condenser in two parallel streams. The flow of steam is split into these two streams, so the power plant can work using wet, dry or both cooling systems at a time. As has been mentioned for the NGCC case, the hybrid cooling simulation has two design cases. Due to the efficiency loss of the air-cooled condenser in warm and dry conditions, during those months of the year when the ambient temperature is too high to let the dry cooling system work efficiently, only wet cooling will be used to condense the steam. This is done by circulating the 100% of the steam mass flow through the stream going through wet cooling. Alternatively, the totality of the steam mass flow will go through the air-cooled condenser in colder months. This means that the description of the power plant using hybrid cooling will be the same as the descriptions of the power plants using wet and dry cooling depending on the time of the year and the cooling system chosen.

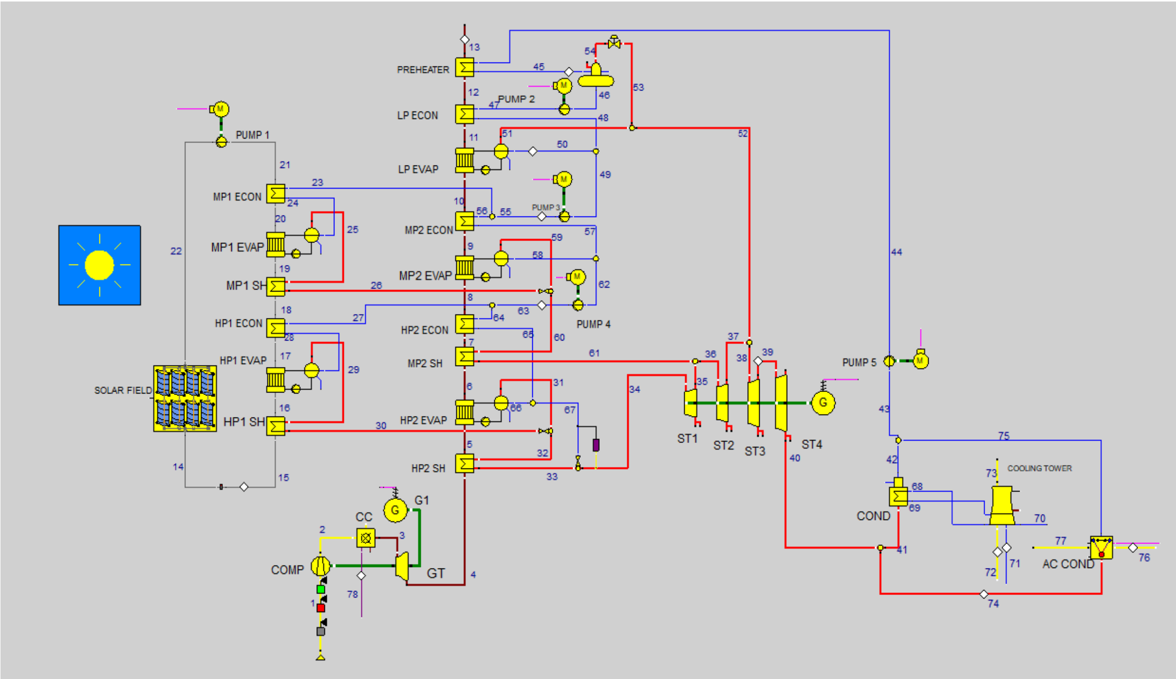

Figure 9. CSP integrated combined cycle power plant with hybrid cooling system

3.2.4. The CSP integrated combined cycle dynamic simulation

A dynamic simulation has been made in a way that the power plant can be analysed through a whole year of operation. Hourly temperatures and DNI data in Sevilla from 2005 to 2009, both years included, have been used to calculate the hourly mean of a whole year. The data used as input for the sun is not real 2017 data, but a mean computed from real data of five whole years. After the time series have been simulated, it is possible to get graphs of different power plant characteristics throughout the year, such as total power output, efficiency or effective heat from the CSP field.

The diagrams obtained from the time series simulation present a constantly changing pattern, which is due to the 0 W/m^2 DNI during night hours. When the DNI is equal to 0, the power output contribution of the solar field is 0 as well, which results in a lower steam turbine power output. As the total P_{out} has been set, the gas turbine output power must be necessarily higher for this night hours in order to meet the requirements. This has as a result higher mass flow of fuel (in the combustion chamber inlet) and zero mass flow of oil in stream 22, which is the stream of thermal oil going into the CSP field.

When it comes to the weather conditions, now putting aside the night hours effect, the analysis of the diagrams is done looking at how maximum and minimum values of the different parameters vary over a year. Looking at the ambient temperature variation during the year, warmest months are observed to be July, august and September. Also, it can be appreciated how the DNI reaches its highest values during warm months (summer season: June, July, August, September…), even if it does not show significant variations during the year.

Solar heat of the solar field reaches highest points in warm months, when the DNI is also higher (June, July, August…). This is also related with a higher mass flow in stream 22 during these months, as well as higher optical, thermal and overall solar field efficiency.

The solar field contributes to make the steam turbine power output higher, so in warmer and sunnier months, steam turbine power output also reaches its highest values.

Due to the higher power output of the solar field during summer months, the output of the gas turbine is lower these months. This is explained because, in order to get to the desired total output power of the plant, when there is more contribution of the solar field, the power needed from the gas turbine would be lower as well. Consequently, there is a lower mass flow of fuel in the combustion chamber inlet, which leads to a higher combined cycle efficiency.

Fuel mass flow has a constant maximum throughout the year, as it is reached during night time every day. In this case what makes sense is looking at its minimum values, reached, as was stated before, during warm sunny months. In summer months, the CSP field is working at its maximum capacity during day time, injecting steam into the HRSG of the combined cycle. Due to this additional steam production, the steam turbine is going to have a higher output power, thus requiring less power output from the gas turbine and needing less fuel mass flow injected to the combustion chamber.

4. RESULTS

4.1. EXERGETIC ANALYSIS

An exergetic analysis relies on the concept of 'exergy', which is defined as the total work potential or maximum useful work available of a given system in a determined environment. Exergy can be destroyed and is a characteristic of both system and environment but can be seen as an extensive property of the system alone once the environment has been properly defined. The information this analysis gives is how much of that work potential or exergy has been consumed by a process, usually referred as exergy destroyed. The exergy destroyed is also called irreversibility and is inversely proportional to a process efficiency, so the exergy analysis is giving information about a process overall performance [40]. When applied to each of a power plant's component, this analysis is highly useful to determine the exergy destroyed related costs (later analysed in an exergoeconomic analysis), an locate the causes of this inefficiencies, that can be either avoidable (eliminated by technical improvements) or unavoidable (due to the plant structure and how its components interact together) [41][42].

In this work, a matlab script is used to perform the exergetic analysis of each plant. Exergy balances are written at the component level.

In the exergetic analysis the exergy of fuel (E_F), exergy of product (E_P) and exergy destruction (E_D) of each component of the power plant are calculated. The fuel represents the expense of resources to get a certain product, while the product is the desired outcome of the thermodynamic process [41]. The exergetic efficiency is the ratio between exergy of product and fuel and it is defined both at the component and at the plant level. In order to estimate the E_F and E_P of each component, the total exergy of each stream is needed. The total exergy is obtained from the sum of physical and chemical exergy of each stream, computed from the stream values in Ebsilon.

4.1.1. The NGCC power plant

Table 3. Results of the exergetic analysis for the NGCC simulation

	Wet cooling simulation	**Dry cooling simulation**
ε_{tot} (%)	57.33	56.40
$\dot{E}_{F\ tot}$ (MW)	762.72	775.59
$\dot{E}_{P\ tot}$ (MW)	437.27	437.45
$\dot{E}_{D\ tot}$ (MW)	313.95	317.36
$y_{D\ tot}$(%)	41.16	40.92

Exergetic analysis results show higher exergetic efficiency for the simulation using wet cooling (57.3%) than for the one using an air-cooled condenser (56.4%). The reason to have a lower efficiency when using dry cooling is the power input needed to work the fan, which implies a higher fuel consumption in order to get to the desired power output. Total $\dot{E}_F$ is higher for dry cooling again because of this power input in the fan, while $\dot{E}_P$ is practically the same for both simulations, given that they have the same power output, fixed throughout the whole study. The higher $\dot{E}_F$ of the dry cooling simulation and the equal $\dot{E}_P$ of both make the $\dot{E}_D$ of this simulation higher.

When looking at the component-level results, the combustion chamber is identified as the biggest source of thermodynamic inefficiencies in the plant. 29.3% of the total E_F is destroyed in the combustion chamber, which implies a contribution to the total exergy destruction of 71.2 and 71.6% for wet and dry cooling respectively. The exergy destroyed in the combustion chamber is mainly due to the combustion reaction. As the total power output is fixed for all simulations, the simulations including an air-cooled condenser and needing a power input for the fan, will need a higher mass flow of fuel in the combustion chamber. In this way a slightly higher gas turbine output is achieved, and the total power output requirement is met. This explains why exergy destruction in the combustion chamber is slightly higher for the simulations using dry cooling (227.2 MW) than for the one using wet cooling (223.4 MW). The next component in exergy destruction contribution is the expander of the gas turbine system, with 3.2% of the total $\dot{E}_F$ destroyed (7.7% of the total exergy destruction) for both simulations. Exergy destruction within the gas turbine is mostly due to friction. A higher mass flow of flue gases going through the gas turbine increases the effect of friction in exergy destruction. This makes exergy destruction within the expander slightly higher in the dry cooling simulation, due to a higher mass flow of fuel at the combustion chamber inlet. In the dry cooling simulation, the exergy destruction within the air-cooled condenser is considerably high compared to other components, explained by the fan power input, increasing in this way the $\dot{E}_F$ that would otherwise be zero. Among the rest of the components, HRSG is next in exergy destroyed, this time mainly related to heat transfer, followed by the compressor.

The least efficient components from an exergetic point of view are the combustion chamber (70.7 %) and some components within the HRSG, especially the intermediate-pressure superheater (35.5%), the intermediate-pressure economizer (68.3%), the low-pressure superheater (68.3%) and the low-pressure economizer (65.4%).

The simulation using hybrid cooling is not considered separately in this part. During warmer months, when the hybrid cooling system is working as wet cooling, the power plant shows the exact same exergetic analysis as the one for the wet cooling simulation. Same happens for colder weather, when the hybrid cooling system works in dry mode, the power plant exergetic analysis will have the same results as those of the dry cooling simulation.

4.1.2. The CSP integrated combined cycle power plant

Table 4. Results of the exergetic analysis for the CSP integrated combined cycle simulation

	Wet cooling simulation		**Dry cooling simulation**	
	Combined cycle	Combined cycle + CSP field	Combined cycle	Combined cycle + CSP field
ε_{tot} (%)	73.79	51.02	68.68	48.55
$\dot{E}_{F\ tot}$ (MW)	591.52	855.51	636.44	900.42
$\dot{E}_{P\ tot}$ (MW)	436.50	436.50	437.12	437.12
$\dot{E}_{D\ tot}$ (MW)	155.37	419.36	156.99	420.98
$y_{D\ tot}$(%)	26.27	49.02	24.67	46.75

The exergetic efficiency of the CSP integrated combined cycle using wet cooling is 51.02%, higher than that of the simulation using dry cooling (48.55%), again because of the higher mass flow of fuel needed to compensate the power input to work the air-cooled condenser fan. However, if to calculate the total fuel exergy of the plant, the $\dot{E}_F$ of the solar field is dismissed (263.99 MW), the exergetic efficiency of the combined cycle is obtained, with values 73.79 and 68.68% for wet and dry cooling, respectively. This higher value compared to the NGCC power plant is due to the lower fuel mass flow needed to achieve the required power output, as the CSP field is contributing to achieve such output in this case (design simulation assuming solar DNI of 950 W/m^2). There is a bigger difference between the exergetic efficiencies of the power plants using wet and dry cooling than there was in the NGCC power plants. This is mainly due to the lower efficiency of the air-cooled condenser because of the hot weather in the static simulation (33.4°C), as well as the higher mass flow of steam to be condensed, needing a considerably higher power input to work the fan. The total $\dot{E}_F$ of the plant is lower if the $\dot{E}_F$ of the solar field is dismissed because of the lower mass flow of fuel used. Again total $\dot{E}_F$ is higher for the simulation using dry cooling due to the air-cooled condenser fan power input. Total $\dot{E}_P$ show similar values in both NGCC and CSP integrated combined cycle simulations, and for both wet and dry cooling simulations because of the same power output required for all the simulations. Total $\dot{E}_D$ is higher for the dry cooling simulation due to the higher $\dot{E}_F$ and almost equal $\dot{E}_P$.

At the component level, the combustion chamber shows the highest exergy destroyed (same as in the NGCC simulation) with 28.94 and 28.36% of the total $\dot{E}_F$ destroyed in this component for wet and dry cooling respectively. The $\dot{E}_D$ within the combustion chamber is higher when using dry cooling, again due to the higher fuel mass flow. If the solar field is taken into account, it is next in exergy destruction due to its high $\dot{E}_F$, but in this case this $\dot{E}_D$ does not show an important inefficiency compared to other components, as the fuel used is the sun and it is not associated with any cost. Next components in exergy destruction are the GT expander and the cooling system components (condenser and cooling tower in wet cooling, and air-cooled condenser in dry cooling). In both HRSGs the exergy destroyed in the HP level is higher than that of the IP and LP levels, mainly because of the higher temperatures in the hot side of the heat exchanger, which increases the heat transfer.

The simulation with hybrid cooling system works alternating wet and dry cooling mode. Therefore, the exergy analysis would be the same as those for wet and dry cooling simulations, depending on the time of the year and the weather conditions (dry cooling for colder months and wet cooling for warmer, drier months).

4.2. ECONOMIC ANALYSIS

Costs are calculated for the year 2017, considering it as the actual year. The year of construction start is 2019, while 2021 is considered as the first year of commercial operation of the power plant. The power plant lifetime is considered as 20 years.

4.2.1. The NGCC power plant

Looking at the investment costs of the simulated power plants, wet cooling makes the most economical refrigeration system, as expected. Estimated fixed capital investment (FCI) for NGCC power plant using wet cooling is 204 M€. When substituting the condenser and cooling tower by a dry cooling system, FCI rises to 214 M€. This increment in costs is due entirely to the change in cooling technology and can be even higher if the air-cooled condenser has to work in warmer and drier months. Hybrid cooling implies the highest costs, as it is thought to work either as a wet cooling system or as a dry cooling system depending on the weather conditions, so all components involved in the cooling system need to work at full capacity. Estimated FCI for this simulation is 218 M€. As the power output of the three power plants in set to the same value and considering that dry cooling technology requires a power input for the fan of the air-cooled condenser, the amount of fuel needed to meet the requirements is higher. This makes the cost of fuel higher for the power plant using dry cooling than that of wet cooling. Cost of fuel for the plant using dry cooling is estimated to be 85,3 M€ for mid-2021 (being 2021 assumed to be the first year of commercial operation), while for wet cooling, cost of fuel makes 83,9 M€. Cost of fuel for the power plant using hybrid cooling is variable throughout the year, due to the higher fuel consumption when the power plant is working at dry mode.

At the component level, the highest impact on the total costs of the plant is made by those components involved in the gas turbine system: the expander of the gas turbine, the compressor and the combustion chamber, with a FCI of 32.66 M€, 28.58 M€ and 20.41 M€, respectively. The HRSG also has a high investment cost of 31.21 and 31.75 M€ for wet and dry cooling respectively. The highest contribution to rising costs among the components of the HRSG come from the HPSH, the HPEVAP and the LPEVAP. The steam turbine has a FCI of 22.87 M€, with the highest contribution to costs coming from the LPST (10.07 M€).

The cooling system chosen makes the biggest difference among the costs of the simulations. The FCI of the wet cooling system is 4.18 M€, with condenser and cooling tower costs of 2.02 M€ and 2.16 M€, respectively. The air-cooled condenser has a FCI of 13.63 M€. The hybrid cooling system, therefore, implies a cost that is the sum of both cooling systems: 17.81 M€.

The investment cost rates ($\dot{Z}_k$) in cent/s for the exergoeconomic analysis are computed from the investment costs of the plant components using the following equation:

$$\dot{Z}_k = \frac{(carrying\ charges + O\&M)}{(PEC_{tot} \times \tau)} \times PEC_k \qquad (4.1.)$$

Where PEC is the purchase equipment cost, τ is the annual operating hours (7446 h in this case) and O&M are the operating and maintenance costs. Carrying charges result from the subtraction of O&M and fuel costs to the TRR (total rate of return).

4.2.2. The CSP integrated combined cycle power plant

CSP integrated combined cycle power plants show considerably higher costs than those of a simple combined cycle due to the presence of more power plant components, among which the parabolic trough field implies a quite high rise in costs (160.88 M€), being the component with the highest impact in the plant total costs. CSP technology, despite being quite costly, presents the advantage of saving fuel whenever the ambient conditions make it possible. The Static simulation is made for a summer day, thus making the difference between wet and dry cooling costs even higher than in the NGCC power plant due to the efficiency loss of the air-cooled condenser under these conditions. Estimated FCI for dry and wet cooling power plants are 411 M€ and 385 M€ respectively. Hybrid cooling simulation is designed to be working alternating wet and dry cooling depending on the time of the year and the weather conditions, so costs have been calculated for a system working at full capacity either wet or dry cooling is chosen, making an FCI of 417 M€.

The cooling systems present high differences in costs. The wet cooling system shows a FCI of 6.06 M€ (with condenser and cooling tower FCI of 3.12 M€ and 2.93 M€, respectively), while FCI for the air-cooled condenser is 26.38 M€. This higher cost for the cooling system when compared to the NGCC simulation is due to a higher mass flow of steam to condense, as well as, in the case of the air-cooled condenser, the high cooling air temperature (ambient temperature) in the simulation. Both systems are present in hybrid cooling, so that rises the cooling technology FCI for this simulation to 32.44 M€. Looking at these costs it is easy to draw the conclusion that the overall FCI differences of these power plants are due almost entirely to the cooling system chosen.

At the component level the parabolic trough field implies the highest contribution to total costs, followed by the gas turbine (compressor, combustion chamber and expander), with FCIs of 59.90 and 66.37 M€ for wet and dry cooling respectively. This difference in the gas turbine cost is due to the higher mass flow of fuel needed for the dry cooling simulation. HRSG 1 and 2 make a great impact in the total costs, with FCIs of 21.88 M€

and 34.31/33.55 (wet/dry) M€, respectively. Especially high costs within the HRSGs are found for the HP1EVAP (12.23 M€) and HP2SH (13.26 M€).

Table 5. Investment cost references for the power plant components

Component	Reference
Compressor	[43]
CC	[43]
GT	[43]
SH	[44]
RH	[44]
Evap	[44]
Econ	[44]
Preheater	[44]
ST	[45]
Pumps	[44]
Solar field	[46]
Cond	[44]
Cooling Tower	[45]
AC cond	[46]
Deaerator	[44]

4.3. EXERGOECONOMIC ANALYSIS

The exergoeconomic analysis couples the exergetic analysis with costs. The total costs for each component are calculated by summing up the exergy destruction cost rate ($\dot{C}_{D,k}$) and the investment cost rate ($\dot{Z}_k$). The higher the total cost of a certain component, the bigger its impact on the plant. Components with high total costs are likely to require a separate study of their inefficiencies in order to carry out any improvement.

The exergoeconomic factor (f_k) and relative cost difference (r_k) of each component are calculated using the following equations.

$$f_k = \frac{\dot{Z}_k}{\dot{C}_D + \dot{Z}_k} \tag{4.2.}$$

$$r_k = \frac{c_{p,k} - c_{f,k}}{c_{f,k}} \tag{4.3.}$$

f_k is an indicator of the contribution of $\dot{C}_{D,k}$ and $\dot{Z}_k$ to the total cost of each component ($\dot{C}_{D,k} + \dot{Z}_k$). High values of f_k indicate a high $\dot{Z}_k$, implying that reducing investment costs within a particular component should be considered. A low f_k value implies a high $\dot{C}_{D,k}$, so a reduction in exergy destruction within that component is what must be considered in this case. f_k is considered separately for each power plant component type, as a f_k that is high for a heat exchanger might be normal for a pump. r_k is an indicator of the difference between specific cost of product ($c_{p,k}$) and specific cost of fuel ($c_{f,k}$) [44].

4.3.1. The NGCC power plant

The total $\dot{C}_D$ of the power plant is found to be higher for the simulation using dry cooling, with 240.7 cent/s, while the wet cooling simulation has a total $\dot{C}_D$ of 238.1 cent/s. This is mainly due to the exergy destruction within the air-cooled condenser, making total exergy destruction higher and, therefore, increasing the $\dot{C}_D$. Total investment cost rate is also higher for the power plant using dry cooling than that of the wet cooling simulation, with 169.5 and 162.3 cent/s respectively. The reason to this difference is mainly found in the high investment cost of the air-cooled condenser compared to that of the condenser and cooling tower system.

When looking at the component-level results, the highest $\dot{C}_{D,k}$ is found in the wet cooling simulation dissipative components: condenser and cooling tower. Both simulations show a high combustion chamber $\dot{C}_{D,k}$, being the highest one for the dry cooling simulation. This can be explained by the high exergy destruction within this component. The combustion chamber shows one of the highest $\dot{Z}_k$ of the plant in both simulations, but it is low compared to its $\dot{C}_{D,k}$. The expander of the GT system, the compressor and the LPST are next in $\dot{C}_{D,k}$ and total cost, in that order, with investment cost rates higher for the compressor and the GT than for the LPST. Within the HRSG, there is a higher $\dot{C}_{D,k}$ in the high-pressure level, which can be explained by the fact that the exergy destruction in that same pressure-level is higher too. Besides that, the investment costs rates for the HPHRSG are also higher, increasing the total costs as well, and therefore highlighting the importance of this component.

f_k is higher than usual in the HPSH and IPEVAP within the HRSG, which means a reduction in investment costs should be considered for these components. The combustion chamber f_k is low due to the high $\dot{C}_{D,k}$ compared to the $\dot{Z}_k$, caused by the high exergy destruction in this component. Regarding the cooling system, the air-cooled condenser in the dry cooling simulation has a high f_k due to its high investment cost, so a reduction in it may be considered. The condenser and cooling tower of the wet cooling system show a low f_k due to its high $\dot{C}_{D,k}$ compared to its $\dot{Z}_k$.

r_k shows higher values for pumps, where a power input is necessary to get the desired product, thus raising the cost of product. Negative values of r_k are observed in the cooling system dissipative components (cooling tower, condenser and air-cooled condenser), as their cost of product is zero.

For the hybrid cooling simulation, in this case, the exergoeconomic analysis will show different results than that of the other two simulations, as it includes costs for both wet and dry cooling systems. Total $\dot{C}_D$ and $\dot{Z}$ for this simulation are therefore higher than that of the other two, with 242.2 and 172.5 cent/s, respectively.

The cost of electricity (COE) is 6.10, 6.24 and 6.23 cent/kWh for wet, dry and hybrid cooling simulations respectively. This COE is related with both the investment and the fuel use of each power plant. Calculations show 77% of the total COE comes from the fuel consumption, while only 23% is due to the investment. Even though the total $\dot{Z}$ is higher for the hybrid cooling power plant, the fuel consumption is reduced, as dry cooling is only used 6 months a year, so the power input in the fan has been reduced to the half of that of dry cooling. However, this fuel reduction does not imply a significant cost of fuel variation, as it only involves the cooling system, which makes the COE of the power plant using hybrid cooling slightly lower than that of the power plant using dry cooling.

4.3.2. The CSP integrated combined cycle power plant

The total $\dot{C}_D$ is higher for the simulation using dry cooling (118.97 cent/s) than that of the one with the wet cooling system (117.75 cent/s) due to the higher exergy destruction implied by the air-cooled condenser fan power input. However, total $\dot{C}_D$ is much lower than that of the NGCC power plant, for both wet and dry cooling, mainly because of the lower $\dot{E}_D$. This is due to a lower mass flow of fuel used in this simulation as a result of the contribution of the solar field to the total power output. A lower mass flow of fuel implies lower $\dot{E}_F$ and, considering there is no variation in $\dot{E}_P$, lower $\dot{E}_D$. Total $\dot{Z}$ shows a higher value for dry cooling (304.82 cent/s) than for wet cooling (286.92 cent/s), as the cooling system implies a considerably higher investment cost. Total $\dot{Z}$ is higher in this power plant than it was in the NGCC plant, with a big influence of the solar field, with the highest $\dot{Z}_k$ of the whole plant (132.50 and 130.81 cent/s for wet and dry cooling respectively). Also, the number of components when adding the CSP plant is higher, thus increasing the investment costs.

At the component level, highest $\dot{C}_{D,k}$ is shown by the wet cooling system (condenser and cooling tower), higher than that of the air-cooled condenser. The combustion chamber is next in $\dot{C}_{D,k}$ in the wet cooling plant, while it has the highest $\dot{C}_{D,k}$ in the dry cooling plant, as it is also the component with the highest $\dot{E}_D$. High $\dot{C}_{D,k}$ is shown in the GT expander, followed by the LPST and compressor. $\dot{C}_{D,k}$ for these components in the simulation using dry cooling is higher due to the higher mass flow of fuel used, increasing the mass flow of air and flue gas and making the $\dot{E}_D$ higher owing to the effect of friction. Both $\dot{C}_{D,k}$ and $\dot{Z}_k$ are higher for the HP level than for IP and LP in both HRSG1 and HRSG2.

f_k is lower than usual in the power plant pumps, suggesting the convenience of reducing these components' exergy destruction. A low value of f_k is observed within the combustion chamber, as its $\dot{C}_{D,k}$ highly exceeds its $\dot{Z}_k$. Investment cost reductions should be considered for components of both HRSG1 and HRSG2.

The COE is found to be higher for dry cooling at 6.48 cent/kWh, while the COE for the plant using wet cooling is 6.06 cent/kWh. The reason why the dry cooling simulation has a higher COE than the plant with a wet-recirculating system is related to the air-cooled condenser power input, which implies in this case a bigger difference than in the NGCC due to the additional steam provided by the solar field, which increases the total steam to be condensed. At the same time, the efficiency of the air-cooled condenser is reduced as well due to the high ambient temperature of the design simulation. This time the COE for the hybrid cooling simulation is found to be 6.39 cent/kWh. There is a considerably higher difference between the COE of the plant using dry cooling and the one using hybrid cooling for the CSP integrated combined than there was for the NGCC. The reason for this is again the higher steam mass flow coming from the steam turbine, requiring a higher power input to the air-cooled condenser and, therefore, a higher mass flow of fuel. For the simulation with the hybrid cooling, the fuel used is reduced by half when compared to the simulation with dry cooling, as it only works with the dry cooling technology half of the year. This reduction in fuel mass flow is in this case higher than it was for the NGCC when switching form dry to hybrid cooling and implies a higher difference in the cost of fuel, that lowers the COE of the plant.

4.4. SENSITIVITY ANALYSES

4.4.1. Sensitivity analysis of the cost of water

A sensitivity analysis has been carried out for the NGCC plant and the CSP integrated combined cycle to determine the cost of water in €/m^3 with which the COE of the power plant using wet cooling becomes higher than that of the plants using dry and hybrid cooling. The make-up water of the cooling tower is considered as the only water consumption within the wet cooling system. For the hybrid cooling, the water consumption throughout the power plant lifetime is considered as half the consumption of the wet cooling system, as it is designed to be working with the wet cooling system for half the year.

The NGCC power plant

As has been stated before, the COE for the NGCC plant using wet cooling considering a cost of water of 0 €/m^3 is 6.10 cent/kWh, while the COE for the plant using dry cooling is 6.24€/kWh. Considering that the dry cooling system presents zero water consumption, the COE for this power plant is constant with cost of water variations. Looking at the results shown in Figure 10, a cost of water higher than 1.70 €/kWh would imply a rise in the COE of the NGCC power plant using wet cooling above that of the one using dry cooling. This means that for such water costs, wet cooling is no longer the most economical cooling technology. This happens because the water consumption in the wet cooling technology is high, making the power plant COE highly sensitive to this cost of water variation, while the power plant using dry cooling presents a constant COE. For costs of water above 3.2 €/m^3, the COE for the power plant with wet cooling system is higher than that of the plant using hybrid cooling.

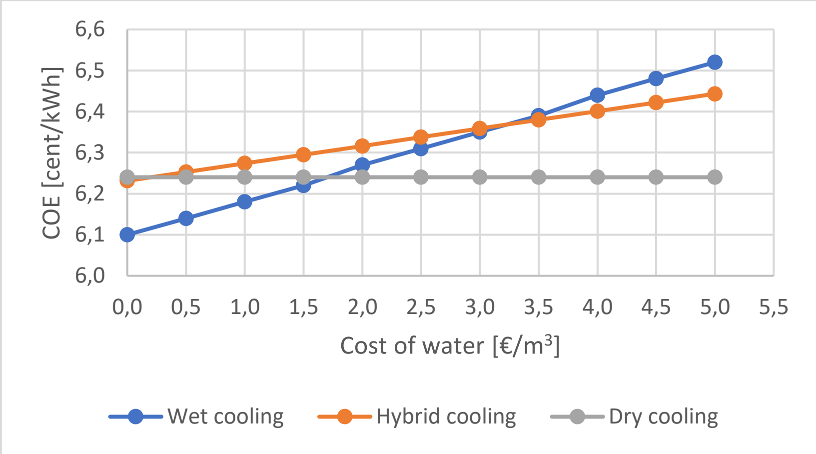

Figure 10. Variation of the COE with the cost of water for the NGCC power plant using different cooling technologies

The CSP integrated combined cycle power plant

The variation of the COE for the CSP integrated combined cycle using wet, dry and hybrid cooling for a cost of water of 0 €/m^3 is 6.06, 6.48 and 6.39 cent/kWh, respectively, as shown in Figure 11. Looking at the results, a cost of water above 2.15 €/m^3 implies a higher COE for the simulation using wet cooling than that with a dry cooling system. The COE shows a bigger sensitivity to cost of water variations than for the NGCC simulation (Figures 12 and 13), mainly due to a higher mass flow of make-up water going into the cooling tower because of the higher mass flow of steam to be condensed. The reason to this higher mass flow of steam is the additional steam produced by the solar field, which is integrated to the steam turbine.

The COE of both power plants using wet cooling and hybrid cooling is affected by cost of water variations. A cost of water higher than 3.4 €/m^3 makes the COE of the simulation with the wet cooling system higher than that of the hybrid cooling one.

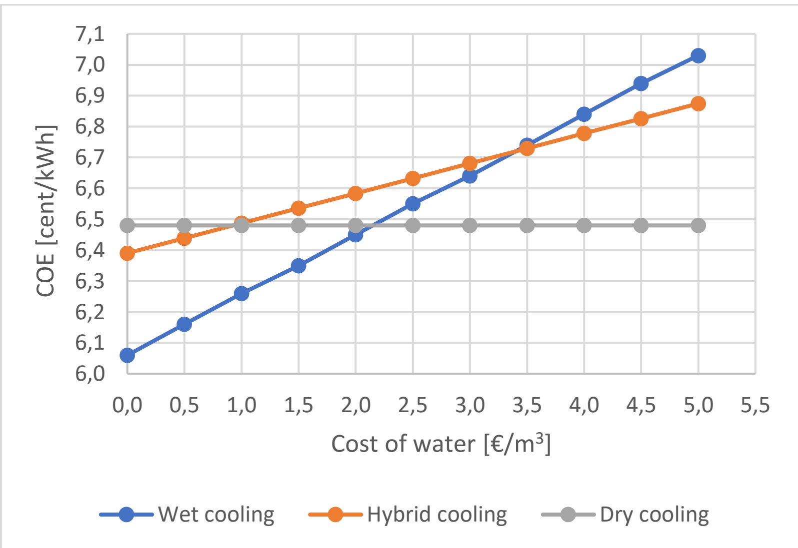

Figure 11. Variation of the COE with the cost of water for the CSP integrated combined cycle using different cooling technologies

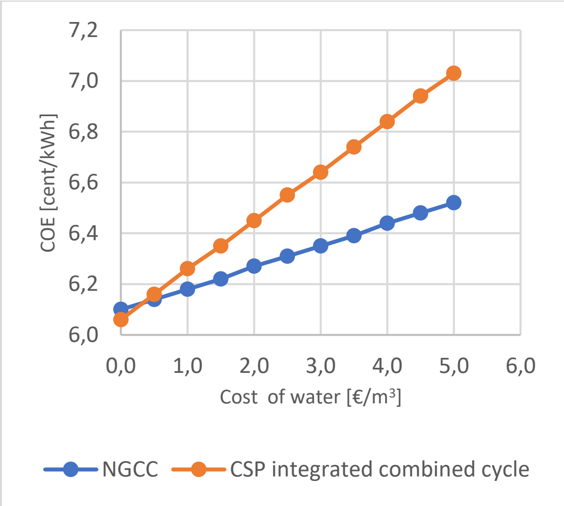

Figure 12. Variation of the COE with the cost of water for the NGCC and the CSP integrated combined cycle using wet cooling

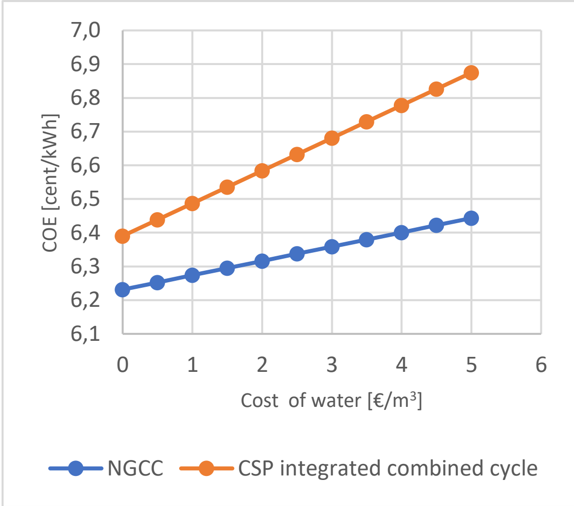

Figure 13. Variation of the COE with the cost of water for the NGCC and the CSP integrated combined cycle using hybrid cooling

4.4.2. Sensitivity analysis of the cost of fuel

Cost of fuel variations from -40% to +40% of the base cost (0.76 cent/MJ) have been made to see the influence of this cost in the COE of the overall power plants. For the plants with hybrid cooling, the fuel consumption is considered as the mean between wet and dry cooling simulations fuel consumption.

The NGCC power plant

For a cost of fuel of -40% of the base cost, both hybrid and dry cooling simulations show the same COE because even if hybrid cooling presents higher investment costs, the cost of fuel for dry cooling is higher. While this cost of fuel increases, it can be appreciated how the dry cooling simulation is slightly more sensitive to these variations due to a higher mass flow of fuel used. Regarding wet cooling, its slope shows also a lower sensitivity to cost of fuel variation than dry and hybrid cooling, as it does not require a power input. Results are shown in Figure 14.

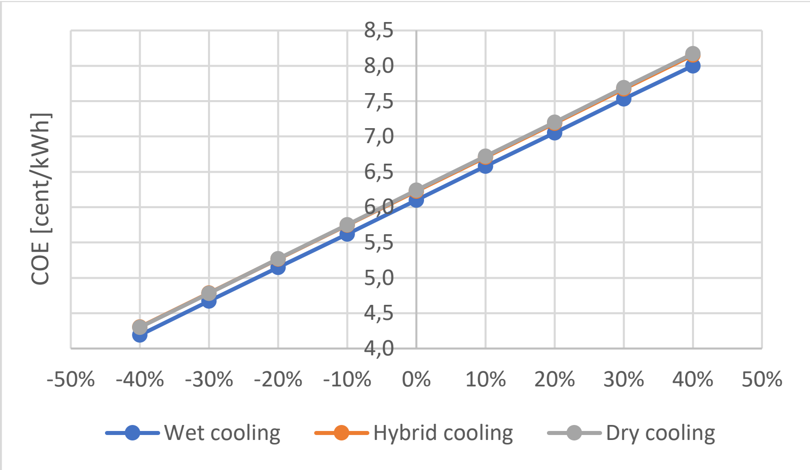

Figure 14. Variation of the COE with the cost of fuel for the NGCC using different cooling technologies

The CSP integrated combined cycle power plant

COE variations with the cost of fuel cause in this plant higher differences among the simulations with different cooling systems. This is because this time the air-cooled condenser needs a higher power input, partly due to its efficiency loss due to warmer weather and partly due to a higher mass flow of steam passing through. The higher the air-cooled condenser power input, the higher the fuel consumption. Variations in the COE with the cost of fuel are directly proportional to the fuel needed to get the desired power output, so the simulation using dry cooling shows higher sensitivity, followed by hybrid cooling. Results are shown in Figure 15.

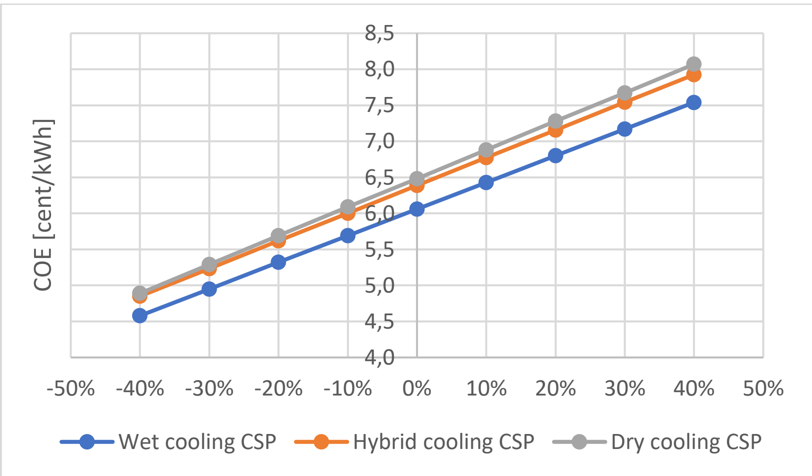

Figure 15. Variation of the COE with the cost of fuel for the CSP integrated combined cycle using different cooling technologies

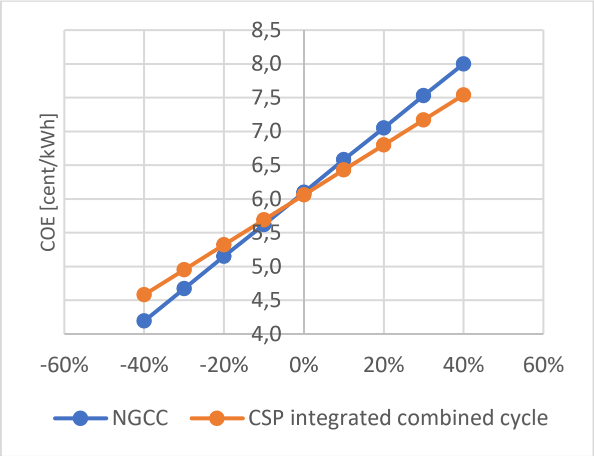

Figure 16. Variation of the COE with the cost of fuel for the NGCC and the CSP integrated combined cycle using wet cooling

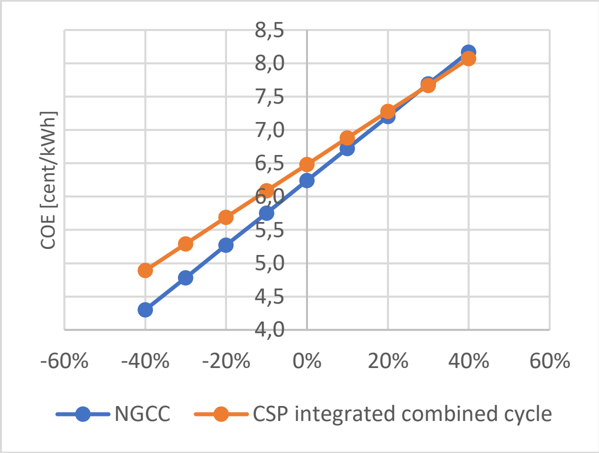

Figure 17. Variation of the COE with the cost of fuel for the NGCC and the CSP integrated combined cycle using dry cooling

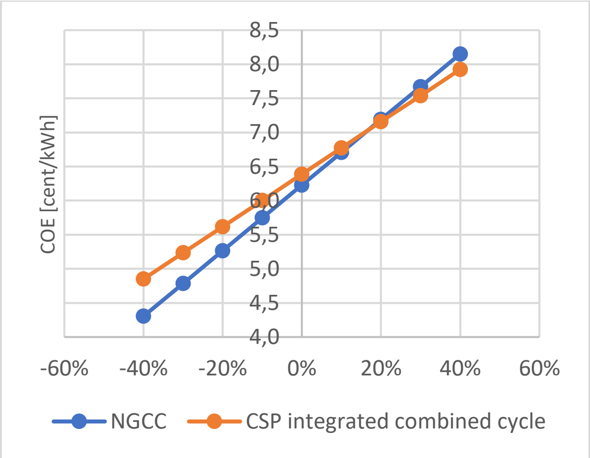

Figure 18. Variation of the COE with the cost of fuel for the NGCC and the CSP integrated combined cycle using hybrid cooling.

5. CONCLUSION

In this work, the performance of two types of power plants (natural gas combined cycle and concentrated solar power integrated combined cycle) using three different cooling systems (wet, dry and hybrid cooling) has been evaluated.

For an equal power output of the power plants simulated, results show that the concentrated solar power integrated combined cycle requires higher water consumption when using wet cooling than the natural gas combined cycle. This is since this power plant relies more on its steam turbine to get the desired output, as the solar field generates additional steam that implies a higher mass flow of cooling water. When using a dry cooling method, the power input needed to work the fan of the air-cooled condenser is also higher in the simulation including the solar field, again because of the higher steam mass flow. In this case the weather conditions under which the concentrated solar power integrated combined cycle has been simulated also influence this higher power input, as the ambient temperature in the summer solstice is high, and this lowers considerably the efficiency of the air-cooled condenser.

The plant including the solar field uses lower amount of fuel than the natural gas combined cycle. The higher portion of the total power output coming from the steam turbine due to the additional steam integrated by the solar field is the reason for this fuel reduction. This lower use of fuel is only accountable during times when there is sun activity, so the power plant needs to work as a simple combined cycle during night time and cloudy days. However, the fuel saved in the power plant implies an important cost reduction in time. This lower fuel mass flow involves a higher combined cycle efficiency for the power plant with the solar field.

When using dry cooling, the water consumption is avoided, but there is an additional need of a power input to work the fan to circulate the air and condense steam. Therefore, there is a need for a higher fuel mass to the combustion chamber. This implies an overall efficiency reduction. The costs implied by the use of the air-cooled condenser are also higher than those of the wet cooling system (condenser and cooling tower).

From an economic point of view, the concentrated solar power integrated combined cycle has a considerably higher fixed capital investment than the natural gas combined cycle. The solar field is the main cause to this investment increase. However, considering the fuel savings of the power plant with the solar field, the cost of electricity for both plants using wet cooling is very similar, with that of the natural gas combined cycle power plant somewhat higher (6.10 cent/kWh and 6.06 cent/kWh for natural gas combined cycle and concentrated solar power integrated combined cycle, respectively). When using dry cooling, however, the plant including the solar field shows a higher cost of electricity (6.48 cent/kWh) than the single natural gas combined cycle (6.24 cent/kWh).

The hybrid cooling technology of this study includes both a wet and a dry cooling system in parallel. The power plant with this technology works differently depending on the weather conditions. In this way, in warm and dry weather, when the air-cooled condenser efficiency is low, the steam to be condensed is fully diverted to the wet cooling system. In colder months, however, the steam is condensed using the air-cooled condenser. It is assumed that the hybrid cooling system uses each of the cooling methods for six months a year.

Hybrid cooling implies in both power plants a cost of electricity higher than the case with wet cooling but still a cost slightly lower than the case with dry cooling (6.23 cent/kWh for natural gas combined cycle and 6.39 cent/kWh concentrated solar power integrated combined cycle). This small difference between the hybrid and dry systems is the result of a higher investment cost in the hybrid case, as it involves both wet and dry cooling technologies. However, since a lower amount of fuel is used in the plant with the hybrid cooling system, compared to the plant with the air-cooled condenser, its overall cost of electricity is somewhat lower.

Variations in the cost of fuel affect the cost of electricity of the natural gas combined cycle power plant more than the concentrated solar power integrated combined cycle. This is because of the higher mass flow used in the natural gas combined cycle. Also, when comparing cooling technologies, the cost of electricity of the power plant using dry cooling presents a higher sensitivity to fuel cost variations than that using wet cooling. This happens because the first involves a higher fuel mass flow to make up for the power input required in the air-cooled condenser.

Variations in the cost of water affect the cost of electricity of the concentrated solar power integrated combined cycle more when using wet or hybrid cooling when compared to the natural gas combined cycle power plant, as there is more steam to be cooled, and therefore, more cooling water. With costs of water above 1.7 €/m^3 for the natural gas combined cycle power plant and 2.15 €/m^3 for the concentrated solar integrated combined cycle, the wet cooling method is no longer an economically viable option against the dry cooling method. Hybrid cooling is considered to use half the annual amount of water than that used in the wet cooling system, so the variation of the power plant cost of electricity using this method is less pronounced than using wet cooling. The sensitivity analysis of the cost of water is giving the information that for high costs of water, dry cooling is the most economical cooling system because of the approximately zero-water consumption in this case, thus considering the convenience of an air-cooled condenser for such costs.

From the results of the above-mentioned analyses, hybrid cooling presents an option that allows higher power plant efficiencies than dry cooling, but with a lower water use than wet cooling. It also presents a lower cost of electricity than dry cooling when low costs of water are considered due to the relatively less fuel needed. It thus arises as a viable future option to consider when designing a cooling system.

Nowadays most power plants use closed wet-recirculating cooling systems with a condenser and cooling tower as their cooling technology. This is mainly because of the relatively higher efficiencies and lower costs of the technology, when compared to dry cooling, and the lower environmental impact when compared to an open-loop system (once-through cooling). However, with rising global water scarcity due to environmental reasons, as well as increasing water consumption, there is a need to consider different cooling options that allow lower water use.

The intention of this work was to serve as an academic text on the role of water and cooling systems in electricity production and reveal the importance of studying and evaluating different cooling options in the future.

Bibliography

[1] F. R. Rijsberman, “Water scarcity: Fact or fiction?,” *Agric. Water Manag.*, vol. 80, no. 1–3 SPEC. ISS., pp. 5–22, 2006.

[2] N. Bieber *et al.*, “Sustainable planning of the energy-water-food nexus using decision making tools,” *Energy Policy*, vol. 113, no. November 2017, pp. 584–607, 2018.

[3] M. Kummu, P. J. Ward, H. De Moel, and O. Varis, “Is physical water scarcity a new phenomenon? Global assessment of water shortage over the last two millennia,” *Environ. Res. Lett.*, vol. 5, no. 3, 2010.

[4] B. Ali and A. Kumar, “Development of life cycle water-demand coefficients for coal-based power generation technologies,” *Energy Convers. Manag.*, vol. 90, pp. 247–260, 2015.

[5] B. R. Scanlon, I. Duncan, and R. C. Reedy, “Drought and the water-energy nexus in Texas,” *Environ. Res. Lett.*, vol. 8, no. 4, 2013.

[6] S. Hadian and K. Madani, “The Water Demand of Energy: Implications for Sustainable Energy Policy Development,” *Sustainability*, vol. 5, no. 11, pp. 4674–4687, 2013.

[7] P. Ganguli, D. Kumar, and A. R. Ganguly, “US Power Production at Risk from Water Stress in a Changing Climate,” *Sci. Rep.*, vol. 7, no. 1, pp. 1–13, 2017.

[8] C. Tan and Q. Zhi, “The energy-water nexus: A literature review of the dependence of energy on water,” *Energy Procedia*, vol. 88, pp. 277–284, 2016.

[9] X. Zhang *et al.*, “China’s coal-fired power plants impose pressure on water resources,” *J. Clean. Prod.*, vol. 161, pp. 1171–1179, 2017.

[10] L. Lin and Y. Chen, “Evaluation of Future Water Use for Electricity Generation under Different Energy Development Scenarios in China,” *Sustainability*, vol. 10, no. 1, p. 30, 2017.

[11] T. Semertzidis, C. Spataru, and R. Bleischwitz, “Cross-sectional integration of the water-energy nexus in Brazil,” *J. Sustain. Dev. Energy, Water Environ. Syst.*, vol. 6, no. 1, pp. 114–128, 2018.

[12] E. A. Grubert, F. C. Beach, and M. E. Webber, “Can switching fuels save water? A life cycle quantification of freshwater consumption for Texas coal-and natural gas-fired electricity,” *Environ. Res. Lett.*, vol. 7, no. 4, 2012.

[13] R. S. Dodder, “A review of water use in the U.S. electric power sector: Insights from systems-level perspectives,” *Curr. Opin. Chem. Eng.*, vol. 5, pp. 7–14, 2014.

[14] A. Miara, “Thermal effluent from the power sector : an analysis of once-through cooling system impacts on surface water temperature,” 2013.

[15] K. Birkinshaw, M. Masri, and R. L. Therkelsen, “Comparison of Alternate Cooling Technologies for U.S. Power Plants: Economic, Environmental, and Other Tradeoffs. Final Report, February 2002,” *Calif. Energy Comm.*, pp. 1–270, 2002.

[16] H. Zhai and E. S. Rubin, “Performance and cost of wet and dry cooling systems for pulverized coal power plants with and without carbon capture and storage,” *Energy Policy*, vol. 38, no. 10, pp. 5653–5660, 2010.

[17] G. A. Thopil and A. Pouris, “A 20 year forecast of water usage in electricity generation for South Africa amidst water scarce conditions,” *Renew. Sustain. Energy Rev.*, vol. 62, pp. 1106–1121, 2016.

[18] A. Liqreina and L. Qoaider, “ScienceDirect Dry cooling of concentrating solar power (CSP) plants , an economic competitive option for the desert regions of the MENA region,” *Sol. Energy*, vol. 103, pp. 417–424, 2014.

[19] E. Rezaei, S. Shafiei, and A. Abdollahnezhad, “Reducing water consumption of an industrial plant cooling unit using hybrid cooling tower,” *Energy Convers. Manag.*, vol. 51, no. 2, pp. 311–319, 2010.

[20] C. Paper, “Feasibility of a hybrid cooling system in a thermal power plant Feasibility of a Hybrid Cooling System in a Thermal Power Plant,” no. February 2008, 2015.

[21] L. H. Logan and A. S. Stillwell, “Probabilistic assessment of aquatic species risk from thermoelectric power plant effluent: Incorporating biology into the energy-water nexus,” *Appl. Energy*, vol. 210, no. August 2017, pp. 434–450, 2018.

[22] C. E. Raptis, M. T. H. Van Vliet, and S. Pfister, “Global thermal pollution of rivers from thermoelectric power plants,” *Environ. Res. Lett.*, vol. 11, no. 10, 2016.

[23] B. R. Scanlon *et al.*, “Marginal costs of water savings from cooling system retro fi ts : a case study for Texas power plants,” 2008.

[24] A. Santhosh, A. M. Farid, and K. Youcef-Toumi, “Real-time economic dispatch for the supply side of the energy-water nexus,” *Appl. Energy*, vol. 122, pp. 42–52, 2014.

[25] S. E. Trabelsi, L. Qoaider, and A. Guizani, “Investigation of using molten salt as heat transfer fluid for dry cooled solar parabolic trough power plants under desert conditions,” *Energy Convers. Manag.*, vol. 156, no. November 2017, pp. 253–263, 2018.

[26] S. Bukhary, S. Ahmad, and J. Batista, “Analyzing land and water requirements for solar deployment in the Southwestern United States,” *Renew. Sustain. Energy Rev.*, vol. 82, no. September 2017, pp. 3288–3305, 2018.

[27] J. Macknick, J. Meldrum, S. Nettles-Anderson, G. Heath, and A. Miara, “Life cycle water use for photovoltaic electricity generation: A review and harmonization of literature estimates,” *2014 IEEE 40th Photovolt. Spec. Conf. PVSC 2014*, pp. 1458–1460, 2014.

[28] Y. Chang, R. Huang, R. J. Ries, and E. Masanet, “Life-cycle comparison of greenhouse gas emissions and water consumption for coal and shale gas fired power generation in China,” *Energy*, vol. 86, pp. 335–343, 2015.

[29] J. Yuan, Q. Lei, M. Xiong, J. Guo, and C. Zhao, “Scenario-based analysis on water resources implication of coal power in Western China,” *Sustain.*, vol. 6, no. 10, pp. 7155–7180, 2014.

[30] A. a. Keller, S. Tellinghuisen, C. Lee, D. Larson, B. Dennen, and J. Lee, “Projection of California’s Future Freshwater Requirements for Power Generation,” *Energy Environ.*, vol. 21, no. 2, pp. 1–20, 2010.

[31] Parliament of Australia, “Water requirements of nuclear power stations,” *Parliam. Libr.*, pp. 0–1, 2006.

[32] M. Basheer and N. A. Elagib, “Sensitivity of Water-Energy Nexus to dam operation: A Water-Energy Productivity concept,” *Sci. Total Environ.*, vol. 616–617, pp. 918–926, 2018.

[33] N. Ding, J. Liu, J. Yang, and B. Lu, “Water footprints of energy sources in China: Exploring options to improve water efficiency,” *J. Clean. Prod.*, vol. 174, pp. 1021–1031, 2018.

[34] M. Hasanuzzaman, A. B. M. A. Malek, M. M. Islam, A. K. Pandey, and N. A. Rahim, “Global advancement of cooling technologies for PV systems: A review,” *Sol. Energy*, vol. 137, pp. 25–45, 2016.

[35] E. Ersayin and L. Ozgener, “Performance analysis of combined cycle power plants: A case study,” *Renew. Sustain. Energy Rev.*, vol. 43, pp. 832–842, 2015.

[36] B. J. Alqahtani and D. Patino-Echeverri, “Integrated Solar Combined Cycle Power Plants: Paving the way for thermal solar,” vol. 169, pp. 1–23, 2016.

[37] F. Magrassi, E. Rocco, S. Barberis, M. Gallo, and A. Del Borghi, “Hybrid solar power system versus photovoltaic plant: A comparative analysis through a life cycle approach,” *Renew. Energy*, vol. 130, pp. 290–304, 2019.

[38] SEIA - Solar Energy Industries Association, “Concentrating Solar Power,” pp. 99–111, 2014.

[39] P. Kurup and C. S. Turchi, “Parabolic Trough Collector Cost Update for the System Advisor Model (SAM),” *Tech. Rep. NREL/TP-6A20-65228 Natl. Renew. Energy Lab.*, no. November, pp. 1–40, 2015.

[40] F. Petrakopoulou, G. Tsatsaronis, T. Morosuk, and A. Carassai, “Conventional and advanced exergetic analyses applied to a combined cycle power plant,” *Energy*, vol. 41, no. 1, pp. 146–152, 2012.

[41] T. J. Kotas, “Introduction,” in *The Exergy Method of Thermal Plant Analysis*, 1985, pp. xvii–xix.

[42] Y. Zhao, S. Wang, M. Ge, Y. Li, and Y. Yang, “Energy and exergy analysis of thermoelectric generator system with humidified flue gas,” *Energy Convers. Manag.*, vol. 156, no. October 2017, pp. 140–149, 2018.

[43] Pequot Publishing Inc. *GTW Handbook* , Volume 25, Southport (CT): Pequot Publishing Inc., 2006.

[44] F. Petrakopoulou “Comparative Evaluation of Power Plants with CO2 Capture: Thermodynamic, Economic and Environmental Performance”, Dissertation, Faculty III - Process Sciences, Technical University of Berlin, Berlin, Germany, 2011.

[45] H. P. Loh, J. Lyons, and I. I. I. Charles W. White, “Process Equipment Cost Estimation, Final Report,” *Other Inf. PBD 1 Jan 2002*, no. January, p. Medium: ED; Size: 410 Kilobytes pages, 2002.

[46] WorleyParsons Group, “FPLE - Beacon Solar Energy Project Dry Cooling Evaluation,” no. FPLS-0-LI-450-0001 Rev B, 2008.

ANNEX A. DYNAMIC SIMULATION RESULTS

Ambient data

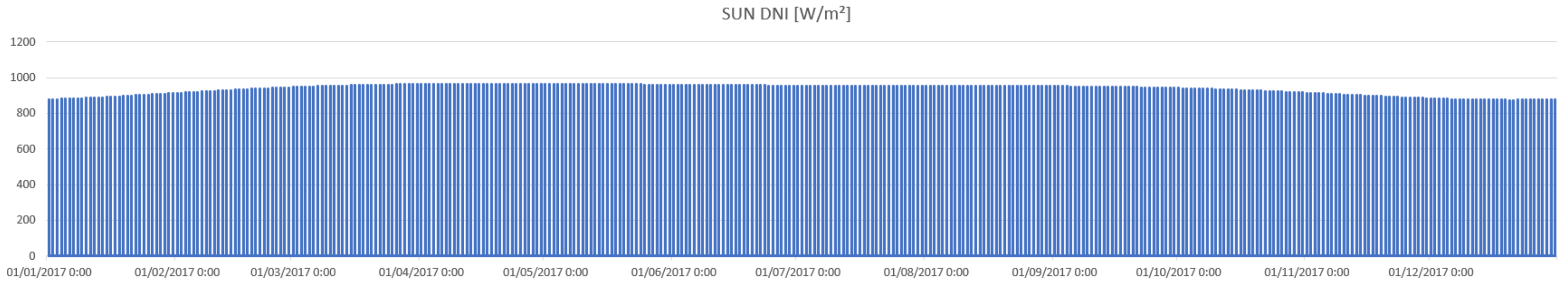

Figure 19. Sun DNI variation throughout the year

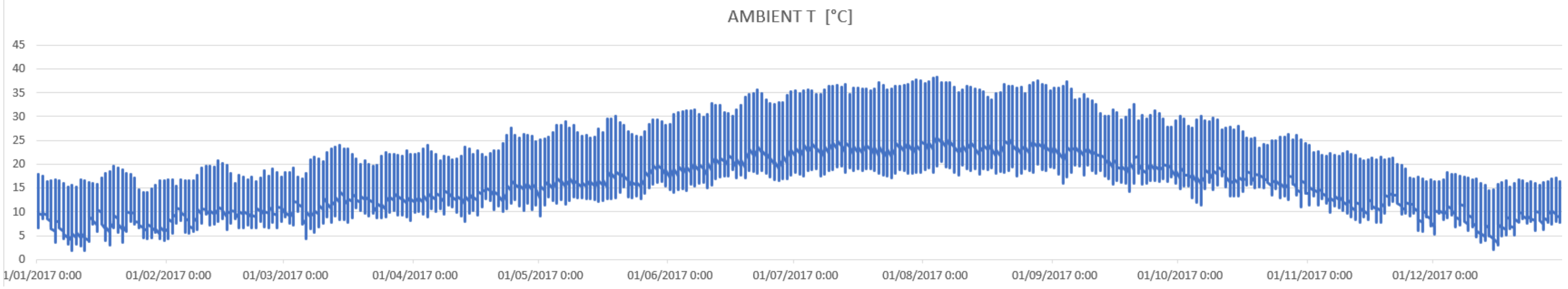

Figure 20. Ambient temperature variation throughout the year

CSP field data

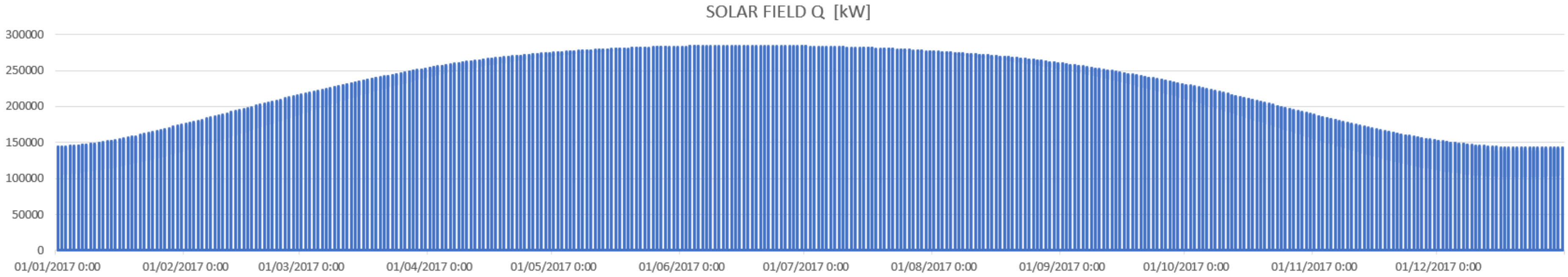

Figure 21. Solar field heat variation throughout the year for the CSP integrated combined cycle power plant

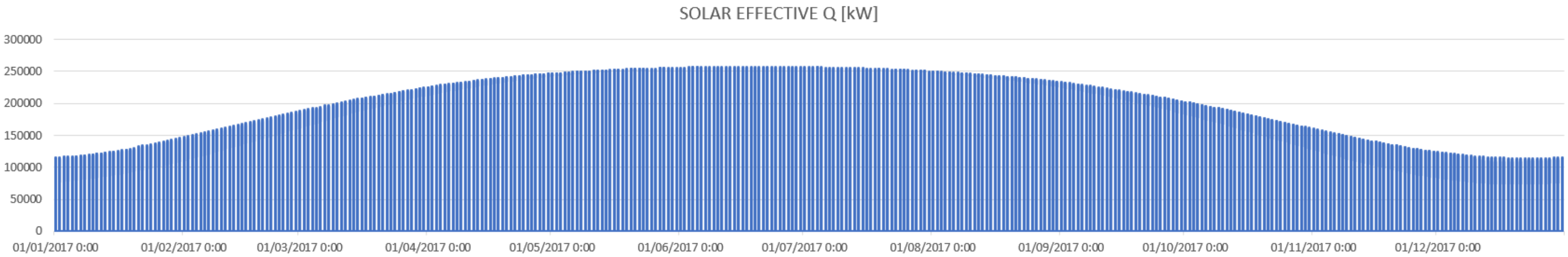

Figure 22.Solar field effective heat variation throughout the year for the CSP integrated combined cycle power plant

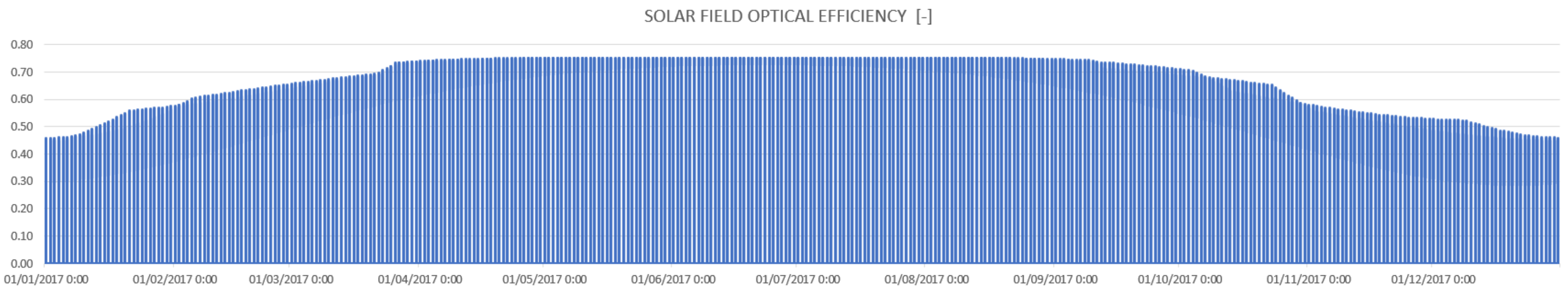

Figure 23. Solar field optical efficiency variation throughout the year for the CSP integrated combined cycle power plant

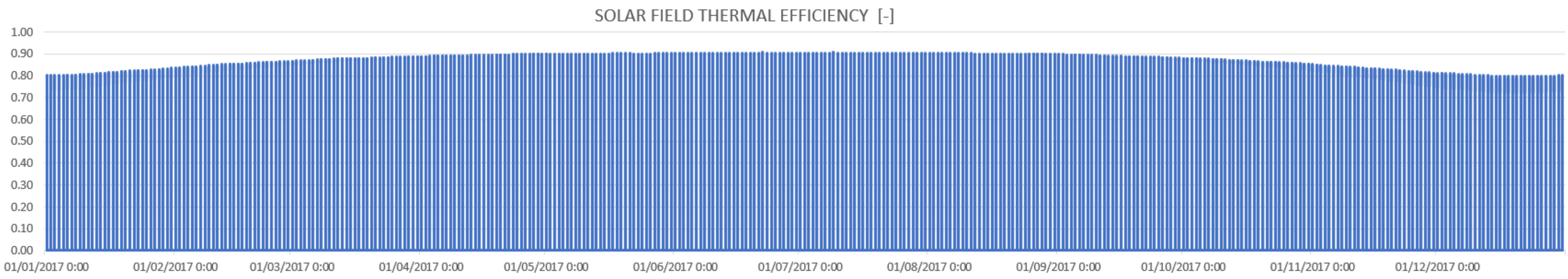

Figure 24.Solar field thermal efficiency variation throughout the year for the CSP integrated combined cycle power plant

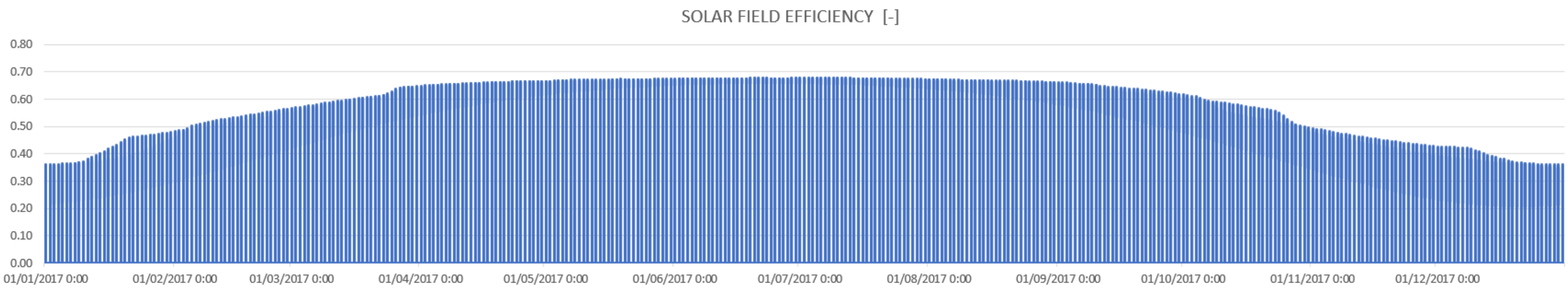

Figure 25. Solar field overall efficiency variation throughout the year for the CSP integrated combined cycle power plant

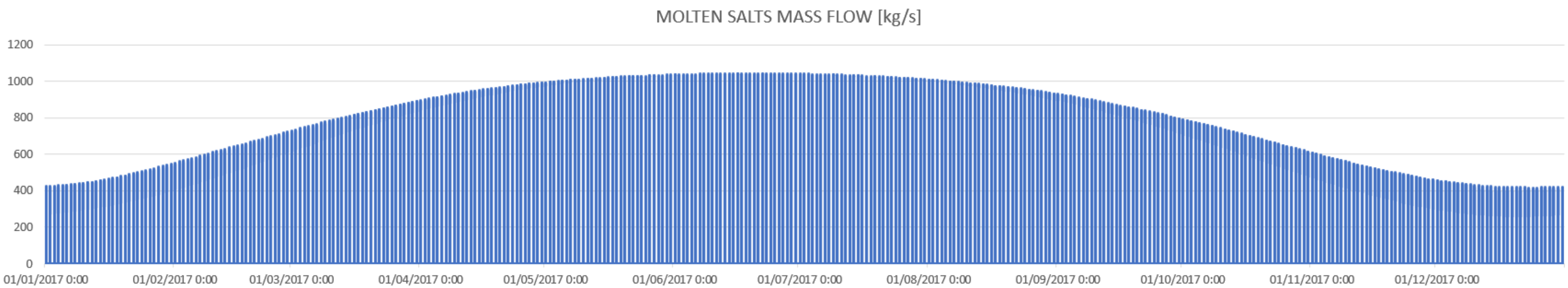

Figure 26. Molten salts mass flow variation throughout the year for the CSP integrated combined cycle power plant

CSP integrated combined cycle simulation using wet cooling

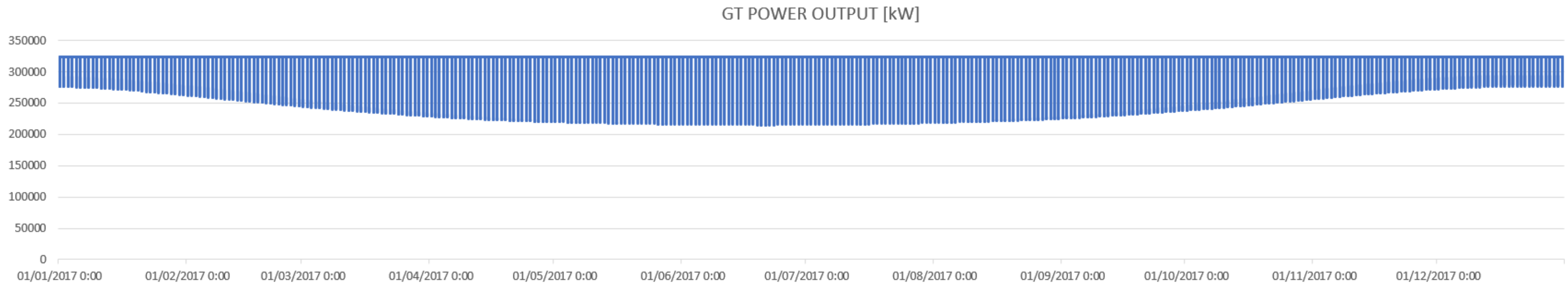

Figure 27. GT power output variation throughout the year for the CSP integrated combined cycle using wet cooling

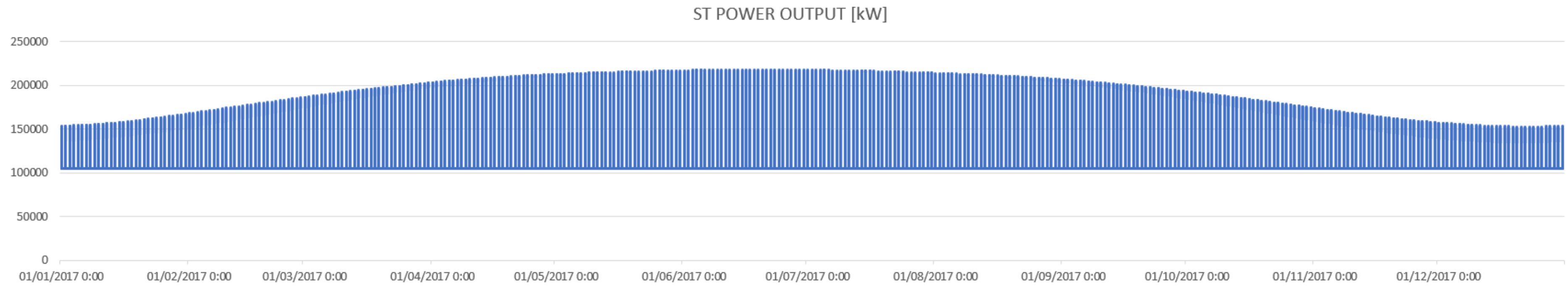

Figure 28. ST power output variation throughout the year for the CSP integrated combined cycle using wet cooling

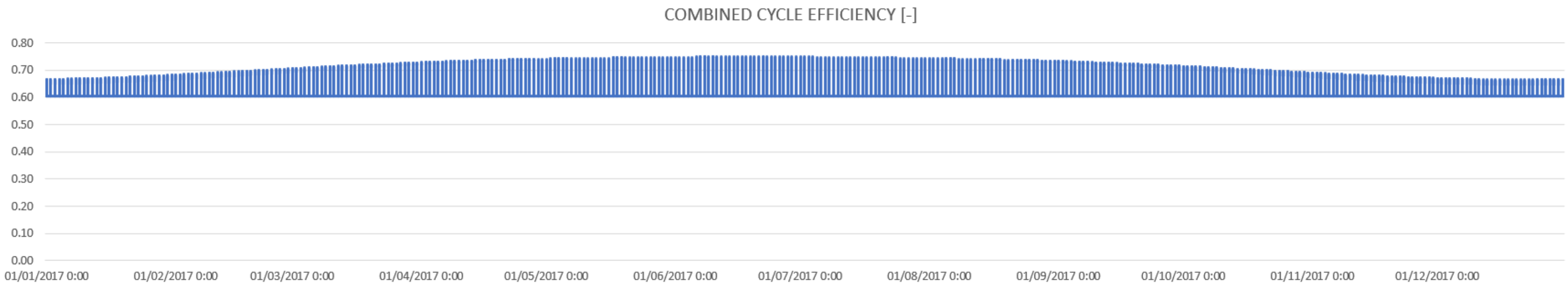

Figure 29. Combined cycle efficiency variation throughout the year for the CSP integrated combined cycle using wet cooling

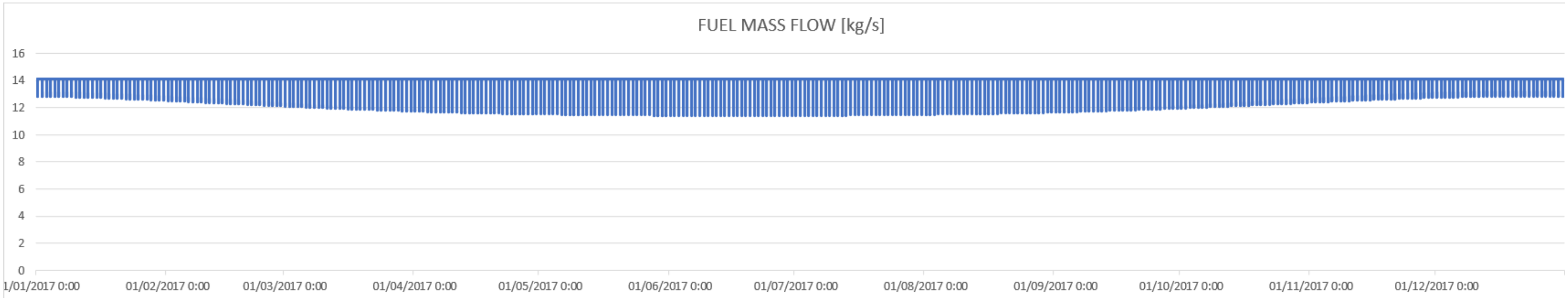

Figure 30. Fuel mass flow variation throughout the year for the CSP integrated combined cycle using wet cooling

CSP integrated combined cycle simulation using dry cooling

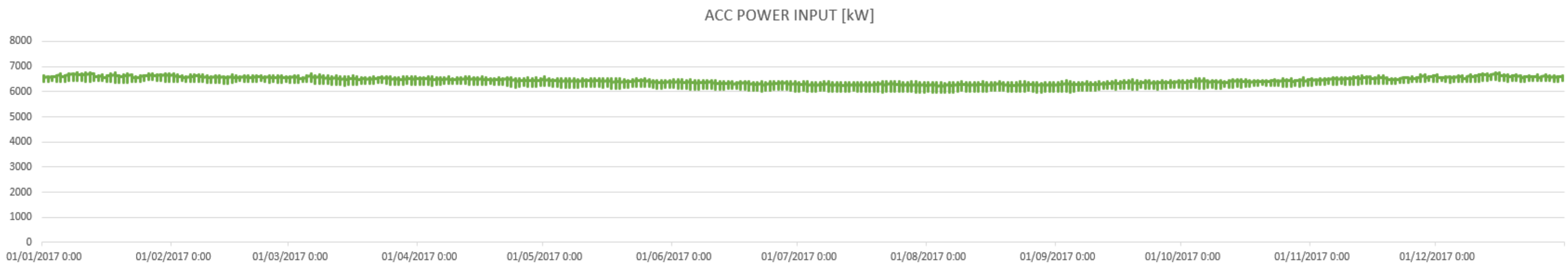

Figure 31. AC condenser power input variation throughout the year for the CSP integrated combined cycle using dry cooling

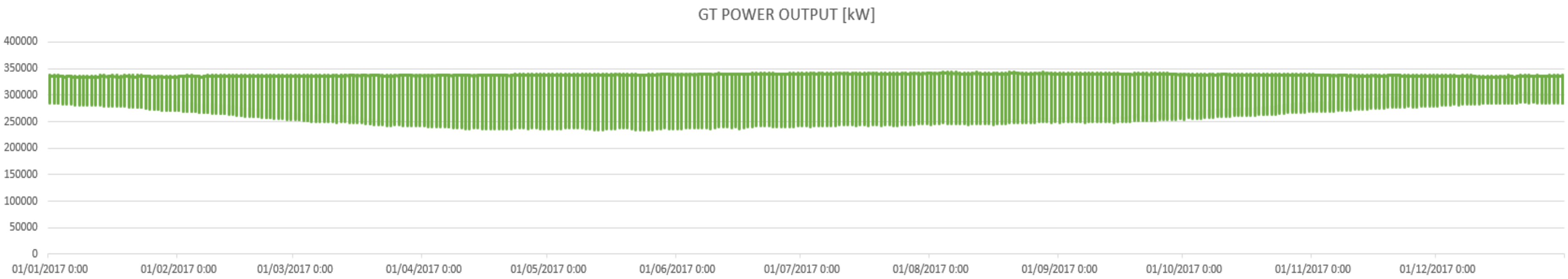

Figure 32. GT power output variation throughout the year for the CSP integrated combined cycle using dry cooling

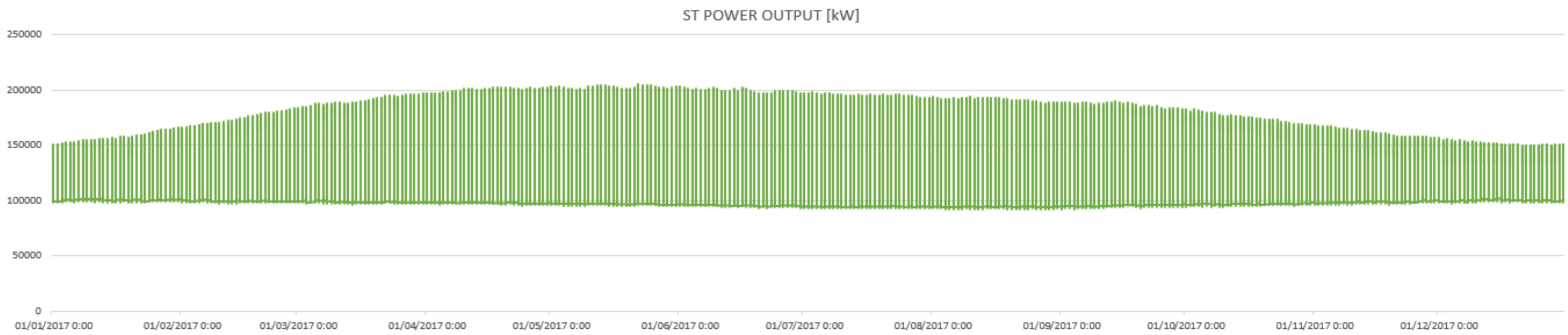

Figure 33. ST power output variation throughout the year for the CSP integrated combined cycle using dry cooling

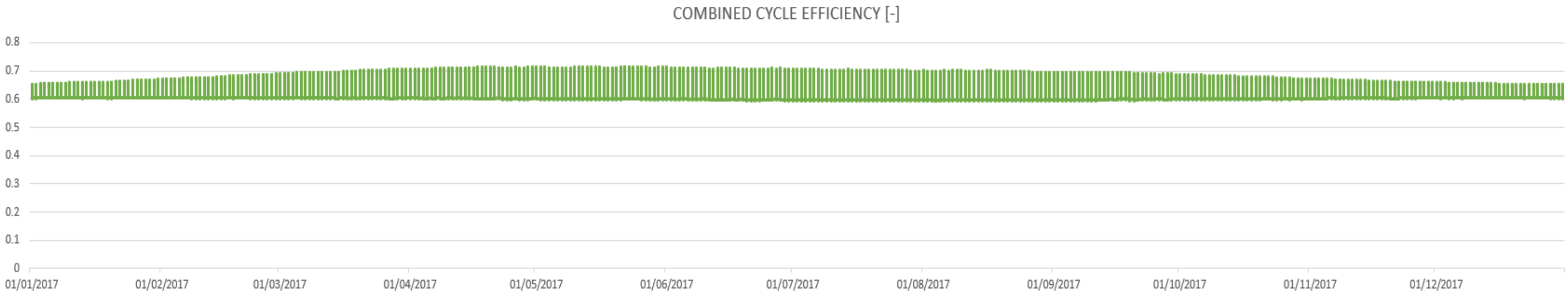

Figure 34. Combined cycle efficiency variation throughout the year for the CSP integrated combined cycle using dry cooling

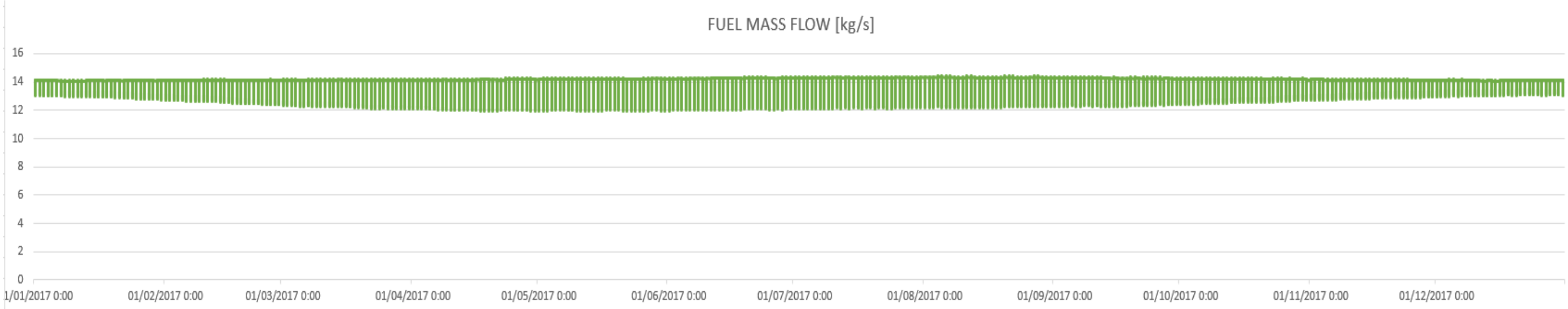

Figure 35. Fuel mass flow variation throughout the year for the CSP integrated combined cycle using dry cooling

ANNEX B. RESULTS AT THE STREAM LEVEL

Table 6. NGCC power plant with wet cooling system results at the stream level

Nr.	$\dot{E}_{PH}$ [MW]	$\dot{E}_{CH}$ [MW]	$\dot{E}_{TOT}$ [MW]	c [Cent/MJ]	$\dot{C}$ [Cent/s]	$\dot{m}$ [kg/s]	T [°C]	p [bar]
1	0	1.06	1.06	0	0	679.09	15.00	1.01
2	258.13	1.06	259.19	1.60	414.15	679.09	398.97	17.00
3	792.08	5.4	797.47	1.28	1017.96	693.75	1239.86	16.50
4	204.13	5.4	209.53	1.28	267.46	693.75	582.98	1.06
5	85.33	2.26	87.59	1.28	111.80	290.00	582.98	1.06
6	46.64	2.26	48.90	1.28	62.42	290.00	397.16	1.05
7	118.8	3.14	121.94	1.28	155.66	403.75	582.98	1.06
8	89.52	3.14	92.66	1.28	118.28	403.75	486.71	1.05
9	135.73	5.40	141.13	1.28	180.70	693.75	449.51	1.05
10	87.46	5.40	92.86	1.28	118.89	693.75	341.49	1.05
11	55.05	5.40	60.45	1.28	77.40	693.75	256.63	1.04
12	54.53	5.40	59.92	1.28	76.72	693.75	255.92	1.04
13	47.80	5.40	53.19	1.28	68.11	693.75	236.74	1.03
14	46.32	5.40	51.72	1.28	66.22	693.75	233.07	1.03
15	44.74	5.40	50.13	1.28	64.19	693.75	229.04	1.02
16	25.27	5.40	30.66	1.28	39.26	693.75	162.21	1.02
17	11.88	5.40	17.27	1.28	22.12	693.75	100.15	1.01
18	80.54	0.18	80.73	1.62	131.14	73.31	330.98	130.21
19	116.51	0.18	116.69	1.61	187.74	73.31	562.98	125.00
20	82.37	0.18	82.56	1.61	132.82	73.31	322.63	25.00
21	90.40	0.20	90.61	1.64	148.76	81.15	314.77	25.00
22	117.16	0.20	117.37	1.61	189.10	81.15	562.98	25.00
23	76.99	0.20	77.19	1.61	124.37	81.15	330.82	5.00
24	95.46	0.26	95.72	1.68	160.97	103.59	305.20	5.00
25	13.57	0.26	13.83	1.68	23.26	103.59	32.87	0.05
26	0.22	0.26	0.48	1.68	0.81	103.59	32.87	0.05
27	0.26	0.26	0.52	1.94	1.01	103.59	32.89	4.00
28	9.02	0.26	9.28	2.24	20.74	103.59	138.00	3.80
29	9.60	0.26	9.86	2.31	22.79	104.37	141.77	3.80
30	7.46	0.20	7.66	2.31	17.72	81.15	141.77	3.80
31	6.74	0.18	6.92	2.31	16.01	73.31	141.77	3.80
32	2.13	0.06	2.19	2.31	5.07	23.21	141.77	3.80
33	2.14	0.06	2.20	2.37	5.20	23.21	141.79	5.05
34	18.24	0.06	18.30	1.92	35.20	23.21	152.21	5.05
35	0.61	0.00	0.61	1.92	1.18	0.78	152.21	5.05
36	17.63	0.06	17.69	1.92	34.02	22.44	152.21	5.05
37	18.71	0.06	18.77	1.95	36.60	22.44	213.07	5.00
38	0.72	0.02	0.74	2.31	1.71	7.83	141.77	3.80
39	0.74	0.02	0.76	2.53	1.92	7.83	142.05	26.36
40	1.75	0.02	1.77	2.26	3.99	7.83	221.70	26.31
41	7.89	0.02	7.91	1.90	15.05	7.83	226.70	26.31
42	8.08	0.02	8.10	1.97	15.94	7.83	246.63	25.00
43	7.82	0.18	8.01	2.43	19.46	73.31	143.41	137.06
44	35.87	0.18	36.05	1.77	63.76	73.31	325.98	130.21
45	0.36	24.32	24.68	6.18	152.47	9736.49	17.26	1.01
46	4.31	24.32	28.63	6.18	176.85	9736.49	22.87	1.01
47	0.00	0.06	0.06	6.18	0.40	25.61	17.26	1.01
48	0.00	0.26	0.26	0.00	0.00	102.82	15.00	1.01
49	0.00	13.8	13.80	0.00	0.00	4868.20	15.00	1.01
50	1.06	7.15	8.21	3.20	26.29	4945.41	21.46	1.01
51	6.18	755.48	761.66	0.76	578.48	14.66	25.00	17.00

Table 7. NGCC power plant with dry cooling system results at the stream level

Nr.	$\dot{E}_{PH}$ [MW]	$\dot{E}_{CH}$ [MW]	$\dot{E}_{TOT}$ [MW]	c [Cent/MJ]	$\dot{C}$ [Cent/s]	$\dot{m}$ [kg/s]	T [°C]	p [bar]
1	0	1.07	1.07	0	0	690.55	15.00	1.01
2	262.49	1.07	263.56	1.59	418.28	690.55	398.97	17.00
3	805.44	5.49	810.93	1.27	1031.54	705.46	1239.86	16.50
4	207.58	5.49	213.06	1.27	271.03	705.46	582.98	1.06
5	85.33	2.26	87.59	1.27	111.41	290.00	582.98	1.06
6	46.05	2.26	48.30	1.27	61.44	290.00	393.95	1.05
7	122.25	3.23	125.48	1.27	159.61	415.46	582.98	1.06
8	92.46	3.23	95.69	1.27	121.72	415.46	487.86	1.05
9	138.02	5.49	143.51	1.28	183.16	705.46	449.51	1.05
10	88.94	5.49	94.42	1.28	120.51	705.46	341.49	1.05
11	55.98	5.49	61.47	1.28	78.45	705.46	256.63	1.04
12	55.45	5.49	60.93	1.28	77.77	705.46	255.92	1.04
13	48.6	5.49	54.09	1.28	69.04	705.46	236.74	1.03
14	47.10	5.49	52.59	1.28	67.12	705.46	233.07	1.03
15	45.49	5.49	50.98	1.28	65.06	705.46	229.04	1.02
16	25.69	5.49	31.18	1.28	39.80	705.46	162.21	1.02
17	12.08	5.49	17.56	1.28	22.42	705.46	100.15	1.01
18	81.90	0.19	82.09	1.62	132.77	74.55	330.98	130.21
19	118.48	0.19	118.66	1.60	189.86	74.55	562.98	125.00
20	83.76	0.19	83.95	1.60	134.32	74.55	322.63	25.00
21	91.93	0.21	92.13	1.63	150.44	82.52	314.77	25.00
22	119.14	0.21	119.35	1.60	191.49	82.52	562.98	25.00
23	78.29	0.21	78.49	1.60	125.94	82.52	330.82	5.00
24	97.07	0.26	97.33	1.67	162.96	105.33	305.20	5.00
25	13.80	0.26	14.07	1.67	23.55	105.33	32.87	0.05
26	0.22	0.26	0.49	1.67	0.82	105.33	32.87	0.05
27	0.27	0.26	0.53	1.93	1.02	105.33	32.89	4.00
28	9.17	0.26	9.43	2.23	21.00	105.33	138.00	3.80
29	9.76	0.27	10.02	2.30	23.05	106.13	141.77	3.80
30	7.59	0.21	7.79	2.30	17.92	82.52	141.77	3.80
31	6.86	0.19	7.04	2.30	16.19	74.55	141.77	3.80
32	2.17	0.06	2.23	2.30	5.13	23.61	141.77	3.80
33	2.17	0.06	2.23	2.35	5.25	23.61	141.79	5.05
34	18.55	0.06	18.61	1.91	35.61	23.61	152.21	5.05
35	0.62	0	0.62	1.91	1.19	0.79	152.21	5.05
36	17.93	0.06	17.98	1.91	34.42	22.81	152.21	5.05
37	19.03	0.06	19.08	1.94	37.02	22.81	213.07	5.00
38	0.73	0.02	0.75	2.30	1.73	7.97	141.77	3.80
39	0.75	0.02	0.77	2.51	1.94	7.97	142.05	26.36
40	1.78	0.02	1.80	2.24	4.04	7.97	221.70	26.31
41	8.02	0.02	8.04	1.89	15.22	7.97	226.70	26.31
42	8.21	0.02	8.23	1.96	16.12	7.97	246.63	25.00
43	7.95	0.19	8.14	2.42	19.67	74.55	143.41	137.06
44	36.47	0.19	36.66	1.76	64.53	74.55	325.98	130.21
45	0.00	85.8	85.80	0.00	0.00	30273.16	15.00	1.01
46	3.21	85.8	89.01	0.53	46.94	30273.16	22.87	1.01
47	6.28	768.23	774.51	0.76	588.24	14.91	25.00	17.00

Table 8. CSP integrated combined cycle power plant with wet cooling system results at the stream level

Nr.	$\dot{E}_{PH}$ [MW]	$\dot{E}_{CH}$ [MW]	$\dot{E}_{TOT}$ [MW]	c [Cent/MJ]	$\dot{C}$ [Cent/s]	$\dot{m}$ [kg/s]	T [°C]	p [bar]
1	0.51	0.77	1.29	0.00	0.00	533.39	33.40	1.01
2	203.88	0.77	204.65	1.52	312.04	533.39	412.78	15.00
3	619.52	4.19	623.71	1.24	776.47	544.75	1231.88	14.50
4	171.57	4.19	175.76	1.24	218.80	544.75	604.99	1.03
5	103.97	4.19	108.17	1.24	134.66	544.75	439.19	1.02
6	69.50	4.19	73.70	1.24	91.75	544.75	340.68	1.02
7	67.69	4.19	71.88	1.24	89.49	544.75	335.35	1.02
8	52.31	4.19	56.50	1.24	70.34	544.75	285.61	1.02
9	45.04	4.19	49.23	1.24	61.29	544.75	260.06	1.02
10	35.80	4.19	39.99	1.24	49.78	544.75	225.39	1.02
11	21.03	4.19	25.23	1.24	31.41	544.75	159.84	1.02
12	20.39	4.19	24.58	1.24	30.60	544.75	157.01	1.02
13	5.48	4.19	9.67	1.24	12.04	544.75	46.10	1.01
14	344.44	3.88	344.44	0.96	330.35	1047.71	395.00	35.00
15	344.44	3.88	344.44	0.96	330.35	1047.71	395.00	35.00
16	329.20	3.88	329.20	0.96	315.74	1047.71	385.48	35.00
17	262.47	3.88	262.47	0.96	251.73	1047.71	340.83	35.00
18	226.05	3.88	226.05	0.96	216.80	1047.71	314.10	35.00
19	224.37	3.88	224.37	0.96	215.19	1047.71	312.82	34.99
20	204.43	3.88	204.43	0.96	196.07	1047.71	297.28	34.99
21	199.48	3.88	199.48	0.96	191.32	1047.71	293.32	34.99
22	201.64	3.88	201.64	0.98	197.85	1047.71	294.31	50.00
23	2.34	0.05	2.40	2.17	5.20	21.87	150.44	40.00
24	6.05	0.05	6.10	1.67	10.19	21.87	247.28	39.95
25	23.04	0.05	23.10	1.35	31.11	21.87	250.28	39.95
26	24.52	0.05	24.58	1.35	33.18	21.87	294.10	39.90
27	15.80	0.24	16.04	2.11	33.83	97.45	181.89	130.00
28	45.96	0.24	46.21	1.53	70.84	97.45	320.83	129.95
29	107.07	0.24	107.31	1.35	144.92	97.45	330.83	129.95
30	120.98	0.24	121.22	1.34	162.92	97.45	375.00	129.90
31	49.74	0.11	49.85	1.58	78.65	45.26	330.68	129.70
32	170.56	0.36	170.92	1.41	241.57	142.71	357.15	129.70
33	234.79	0.36	235.15	1.43	336.65	142.71	594.99	129.65
34	236.51	0.38	236.89	1.45	344.45	153.79	532.00	129.65
35	185.79	0.38	186.17	1.45	270.70	153.79	358.10	39.75
36	219.83	0.46	220.29	1.45	320.03	183.23	351.21	39.75
37	139.92	0.46	140.38	1.45	203.95	183.23	150.30	4.80
38	145.04	0.47	145.51	1.47	213.38	189.79	150.30	4.80
39	96.77	0.47	97.24	1.47	142.59	189.79	99.60	1.00
40	22.42	0.47	22.90	1.47	33.58	189.79	32.87	0.05
41	0.40	0.47	0.88	1.47	1.29	189.79	32.87	0.05
42	0.49	0.47	0.97	1.65	1.60	189.79	32.91	4.55
43	11.77	0.47	12.25	2.07	25.33	189.79	117.01	4.50
44	20.20	0.50	20.70	2.11	43.73	201.58	147.91	4.50
45	20.21	0.50	20.72	2.12	43.86	201.58	147.92	5.05
46	20.74	0.50	21.24	2.12	45.11	201.58	149.84	5.00
47	18.85	0.46	19.31	2.12	41.00	183.23	149.84	5.00
48	1.89	0.05	1.93	2.12	4.11	18.35	149.84	5.00
49	14.39	0.05	14.44	1.83	26.37	18.35	151.84	5.00
50	5.15	0.02	5.16	1.83	9.43	6.56	151.84	5.00
51	9.25	0.03	9.27	1.83	16.94	11.79	151.84	5.00
52	-	-	-	-	-	11.79	149.90	4.50
53	19.61	0.46	20.06	2.17	43.54	183.23	150.44	40.00
54	17.27	0.40	17.67	2.17	38.35	161.35	150.44	40.00
55	24.37	0.40	24.78	2.03	50.39	161.35	180.06	39.80
56	1.14	0.02	1.16	2.03	2.36	7.56	180.06	39.80
57	7.97	0.02	7.98	1.68	13.40	7.56	250.06	39.80
58	32.46	0.07	32.54	1.43	46.58	29.44	281.44	39.8
59	34.08	0.07	34.15	1.44	49.34	29.44	320.68	39.75
60	23.23	0.38	23.62	2.03	48.03	153.79	180.06	39.80
61	24.93	0.38	25.31	2.11	53.39	153.79	181.89	130.00
62	9.13	0.14	9.27	2.11	19.56	56.34	181.89	130.00
63	22.34	0.14	22.48	1.76	39.66	56.34	295.35	129.70
64	17.95	0.11	18.06	1.76	31.86	45.26	295.35	129.70
65	4.39	0.03	4.42	1.76	7.80	11.08	295.35	129.70
66	6.19	40.48	46.67	2.75	128.42	16207.28	22.31	1.01

67	18.86	40.48	59.34	2.75	163.28	16207.28	27.87	0.96
68	0.02	0.15	0.17	2.75	0.46	58.24	22.31	1.01
69	0.55	0.58	1.13	0.00	0.00	233.62	33.40	1.01
70	4.59	22.97	27.56	0.00	0.00	8103.56	33.40	1.01
71	6.48	12.02	18.49	2.01	37.14	8278.93	26.49	1.01
72	4.58	585.66	590.23	0.76	448.28	11.36	25.00	15.00

Table 9. CSP integrated combined cycle power plant with dry cooling system results at the stream level

Nr.	$\dot{E}_{PH}$ [MW]	$\dot{E}_{CH}$ [MW]	$\dot{E}_{TOT}$ [MW]	c [Cent/MJ]	$\dot{C}$ [Cent/s]	$\dot{m}$ [kg/s]	T [°C]	p [bar]
1	0.55	0.83	1.38	0.00	0.00	437.14	33.40	1.01
2	234.27	0.83	235.10	1.51	355.34	437.14	437.15	17.00
3	685.16	4.51	689.66	1.24	855.32	585.91	1251.70	16.50
4	179.67	4.51	184.18	1.24	228.42	585.91	594.64	1.03
5	112.35	4.51	116.86	1.24	144.93	585.91	440.50	1.02
6	74.75	4.51	79.26	1.24	98.30	585.91	340.68	1.02
7	72.82	4.51	77.33	1.24	95.90	585.91	335.39	1.02
8	56.71	4.51	61.21	1.24	75.92	585.91	287.04	1.02
9	48.44	4.51	52.95	1.24	65.67	585.91	260.06	1.02
10	38.97	4.51	43.48	1.24	53.92	585.91	227.12	1.02
11	22.62	4.51	27.13	1.24	33.65	585.91	159.84	1.02
12	21.96	4.51	26.47	1.24	32.82	585.91	157.13	1.02
13	7.79	4.51	12.30	1.24	15.25	585.91	67.07	1.01
14	344.44	3.88	344.44	0.95	326.08	1047.71	395.00	35.00
15	344.44	3.88	344.44	0.95	326.08	1047.71	395.00	35.00
16	329.20	3.88	329.20	0.95	311.66	1047.71	385.48	35.00
17	262.47	3.88	262.47	0.95	248.48	1047.71	340.83	35.00
18	226.05	3.88	226.05	0.95	214.00	1047.71	314.10	35.00
19	224.37	3.88	224.37	0.95	212.41	1047.71	312.82	34.99
20	204.43	3.88	204.43	0.95	193.54	1047.71	297.28	34.99
21	199.48	3.88	199.48	0.95	188.85	1047.71	293.32	34.99
22	201.64	3.88	201.64	0.97	195.27	1047.71	294.31	50.00
23	2.34	0.05	2.40	2.09	5.00	21.87	150.44	40.00
24	6.05	0.05	6.10	1.63	9.92	21.87	247.28	39.95
25	23.04	0.05	23.10	1.32	30.57	21.87	250.28	39.95
26	24.52	0.05	24.58	1.33	32.61	21.87	294.10	39.90
27	15.80	0.24	16.04	2.05	32.86	97.45	181.89	130.00
28	45.96	0.24	46.21	1.50	69.39	97.45	320.83	129.95
29	107.07	0.24	107.31	1.33	142.52	97.45	330.83	129.95
30	120.98	0.24	121.22	1.32	160.29	97.45	375.00	129.90
31	54.22	0.12	54.34	1.56	84.91	49.34	330.68	129.70
32	175.04	0.37	175.40	1.40	245.20	146.79	356.20	129.70
33	238.91	0.37	239.27	1.42	339.30	146.79	584.64	129.65
34	240.43	0.39	240.82	1.44	345.92	156.34	532.00	129.65
35	188.87	0.39	189.26	1.44	271.85	156.34	358.10	39.75
36	224.10	0.47	224.57	1.44	322.39	186.81	351.82	39.75
37	142.65	0.47	143.11	1.44	205.45	186.81	150.30	4.80
38	149.03	0.49	149.52	1.45	217.09	195.00	150.30	4.80
39	99.43	0.49	99.92	1.45	145.07	195.00	99.60	1.00
40	43.32	0.49	43.80	1.45	63.60	195.00	49.42	0.12
41	1.42	0.49	1.90	1.45	2.77	195.00	48.04	0.11
42	1.51	0.49	1.99	1.54	3.06	195.00	48.08	4.55
43	12.12	0.49	12.61	1.94	24.48	195.00	117.13	4.50
44	20.75	0.52	21.27	2.03	43.09	207.06	147.91	4.50
45	20.76	0.52	21.28	2.03	43.22	207.06	147.92	5.05
46	21.30	0.52	21.82	2.04	44.50	207.06	149.84	5.00
47	19.22	0.47	19.69	2.04	40.14	186.81	149.84	5.00
48	2.08	0.05	2.13	2.04	4.35	20.26	149.84	5.00
49	15.89	0.05	15.94	1.80	28.76	20.26	151.84	5.00
50	6.43	0.02	6.45	1.80	11.64	8.20	151.84	5.00
51	9.46	0.03	9.49	1.80	17.12	12.06	151.84	5.00
52	-	-	-	-	-	12.06	149.90	4.50
53	19.99	0.47	20.46	2.09	42.69	186.81	150.44	40.00
54	17.65	0.41	18.06	2.09	37.69	164.93	150.44	40.00
55	24.91	0.41	25.33	1.97	49.98	164.93	180.06	39.80

56	1.30	0.02	1.32	1.97	2.60	8.59	180.06	39.80
57	9.05	0.02	9.07	1.65	15.00	8.59	250.06	39.80
58	33.54	0.08	33.62	1.42	47.62	30.46	280.26	39.8
59	35.27	0.08	35.34	1.43	50.54	30.46	320.68	39.75
60	23.62	0.39	24.01	1.97	47.37	156.34	180.06	39.80
61	25.34	0.39	25.73	2.05	52.72	156.34	181.89	130.00
62	9.55	0.15	9.69	2.05	19.86	58.89	181.89	130.00
63	23.36	0.15	23.51	1.74	40.81	58.89	295.39	129.70
64	19.57	0.12	19.69	1.74	34.19	49.34	295.39	129.70
65	3.79	0.02	3.81	1.74	6.62	9.55	295.39	129.70
66	23.54	117.81	141.35	0.00	0.00	41567.60	33.40	1.01
67	53.56	117.81	171.37	0.57	98.52	41567.60	43.04	1.01
68	5.15	629.90	635.05	0.76	482.32	12.22	25.00	17.00

ANNEX C. RESULTS AT THE COMPONENT LEVEL

Table 10. NGCC power plant with wet cooling results at the component level

Component	$\dot{E}_{F,k}$ [MW]	$\dot{E}_{P,k}$ [MW]	$\dot{E}_{D,k}$ [MW]	$y_{D,k}$ [%]	$y_{D,k}$ * [%]	ε_k [%]	$c_{F,k}$ [Cent/MJ]	$c_{P,k}$ [Cent/MJ]	$\dot{C}_{D,k}$ [Cent/s]	Z_K [Cent/s]	f_K [%]	r_K [%]
Compressor	269.93	258.13	11.8	1.55	3.76	95.63	1.4	1.6	16.55	35.45	68.17	14.29
CC	761.66	538.28	223.38	29.29	71.15	70.67	0.76	1.12	169.66	25.32	12.99	47.37
GT	587.95	563.85	24.09	3.16	7.67	95.9	1.28	1.4	30.75	40.51	56.85	9.38
HPSH	38.69	35.97	2.72	0.36	0.87	93.03	1.28	1.57	3.47	7.2	67.48	22.66
RH	29.28	26.76	2.52	0.33	0.8	91.38	1.28	1.51	3.22	2.97	47.98	17.97
HPEvap	48.27	44.68	3.59	0.47	1.15	92.55	1.28	1.51	4.6	5.58	54.81	17.97
HPEcon	32.41	28.04	4.36	0.57	1.39	86.53	1.28	1.58	5.59	2.79	33.29	23.44
IPSH	0.53	0.19	0.34	0.04	0.11	35.48	1.28	4.78	0.44	0.22	33.33	273.44
IPEvap	6.73	6.14	0.59	0.08	0.19	91.29	1.28	1.8	0.75	2.44	76.49	40.63
IPEcon	1.48	1.01	0.47	0.06	0.15	68.31	1.28	2.05	0.6	0.18	23.08	60.16
LPSH	1.58	1.08	0.5	0.07	0.16	68.27	1.28	2.38	0.64	0.55	46.22	85.94
LPEvap	19.47	16.1	3.36	0.44	1.07	82.72	1.28	1.86	4.31	5.08	54.10	45.31
LPEcon	13.39	8.76	4.63	0.61	1.48	65.4	1.28	2.25	5.93	2.59	30.40	75.78
HPST	34.14	32.25	1.89	0.25	0.6	94.47	1.61	1.91	3.04	6.55	68.30	18.63
MPST	40.18	37.97	2.2	0.29	0.7	94.51	1.61	1.89	3.55	7.22	67.04	17.39
LPST	81.89	74.55	7.33	0.96	2.34	91.05	1.68	1.99	12.33	10.82	46.74	18.45
P1	0	0	0	0	0	80.27	1.58	39.21	0	0.12	100.00	2381.65
P2	0.02	0.02	0	0	0	80.28	1.58	10.63	0.01	0.17	94.44	572.78
P3	1.35	1.08	0.27	0.03	0.08	80.29	1.58	3.19	0.42	1.32	75.86	101.90
P4	0.05	0.04	0.01	0	0	78.35	1.58	4.92	0.02	0.12	85.71	211.39
Cond	-	-	9.41	1.23	3	-	22.46	-	211.24	1.92	0.90	-
Cooling Tower	-	-	9.72	1.27	3.1	-	24.38	-	237.02	2.32	0.97	-
Deaerator	0.54	0.51	0.03	0	0.01	93.77	1.92	3.77	0.06	0.87	93.55	96.35
mixer 1	2.2	1.96	0.24	0.03	0.08	89.19	1.61	1.81	0.38	-	-	12.42
mixer 2	0.7	0.65	0.05	0.01	0.02	93.18	1.61	1.73	0.08	-	-	7.45
mixer 3	10.53	10.1	0.43	0.06	0.14	95.8	1.28	1.33	0.55	-	-	3.91
TOTAL	762.72	437.27	313.95	41.16	100	57.33	0.76	1.69	238.12	162.30	-	-

Table 11. NGCC power plant with dry cooling results at the component level

Component	$\dot{E}_{F,k}$ [MW]	$\dot{E}_{P,k}$ [MW]	$\dot{E}_{D,k}$ [MW]	$y_{D,k}$ [%]	$y_{D,k}$ * [%]	ε_k [%]	$c_{F,k}$ [Cent/MJ]	$c_{P,k}$ [Cent/MJ]	$\dot{C}_{D,k}$ [Cent/s]	Z_K [Cent/s]	f_K [%]	r_K [%]
Compressor	274.49	262.49	12	1.55	3.78	95.63	1.4	1.59	16.75	35.02	67.65	13.57
CC	774.51	547.36	227.15	29.29	71.57	70.67	0.76	1.12	172.52	25.01	12.66	47.37
GT	597.86	573.37	24.5	3.16	7.72	95.9	1.27	1.4	31.16	40.02	56.22	10.24
HPSH	39.29	36.58	2.71	0.35	0.85	93.1	1.27	1.56	3.45	7.12	67.36	22.83
RH	29.79	27.21	2.58	0.33	0.81	91.35	1.27	1.51	3.28	3.16	49.07	18.90
HPEvap	49.09	45.43	3.66	0.47	1.15	92.55	1.28	1.5	4.67	5.59	54.48	17.19
HPEcon	32.95	28.52	4.44	0.57	1.4	86.53	1.28	1.57	5.66	2.8	33.10	22.66
IPSH	0.54	0.19	0.35	0.04	0.11	35.48	1.28	4.75	0.44	0.22	33.33	271.09
IPEvap	6.84	6.25	0.6	0.08	0.19	91.29	1.28	1.79	0.76	2.45	76.32	39.84
IPEcon	1.5	1.03	0.48	0.06	0.15	68.31	1.28	2.04	0.61	0.18	22.78	59.38
LPSH	1.61	1.1	0.51	0.07	0.16	68.27	1.28	2.37	0.65	0.55	45.83	85.16
LPEvap	19.8	16.38	3.42	0.44	1.08	82.72	1.28	1.85	4.37	5.09	53.81	44.53
LPEcon	13.62	8.9	4.71	0.61	1.48	65.4	1.28	2.24	6.01	2.59	30.12	75.00
HPST	34.71	32.8	1.92	0.25	0.6	94.47	1.6	1.89	3.07	6.47	67.82	18.13
MPST	40.86	38.61	2.24	0.29	0.71	94.51	1.6	1.88	3.6	7.13	66.45	17.50
LPST	83.27	75.81	7.46	0.96	2.35	91.05	1.67	1.98	12.48	10.69	46.14	18.56
P1	0	0	0	0	0	80.26	1.57	38.58	0	0.12	100.00	2357.32
P2	0.02	0.02	0	0	0	80.28	1.57	10.48	0.01	0.17	94.44	567.52
P3	1.37	1.1	0.27	0.03	0.09	80.29	1.57	3.16	0.42	1.32	75.86	101.27
P4	0.05	0.04	0.01	0	0	78.36	1.57	4.86	0.02	0.12	85.71	209.55
AC cond	107.06	-	17.57	2.26	5.53	-	0.32	-	5.59	12.86	69.70	-100.00
Deaerator	0.55	0.51	0.03	0	0.01	93.77	1.91	3.71	0.07	0.86	92.47	94.24
mixer 1	2.24	2	0.24	0.03	0.08	89.19	1.6	1.8	0.39	-	-	12.50
mixer 2	0.71	0.66	0.05	0.01	0.02	93.18	1.6	1.72	0.08	-	-	7.50
mixer 3	11.17	10.69	0.48	0.06	0.15	95.69	1.27	1.33	0.61	-	-	4.72
TOTAL	775.59	437.45	317.36	40.92	100	56.4	0.76	1.73	240.7	169.53	-	-

Table 12. CSP integrated combined cycle power plant with wet cooling results at the component level

Component	$\dot{E}_{F,k}$ [MW]	$\dot{E}_{P,k}$ [MW]	$\dot{E}_{D,k}$ [MW]	$y_{D,k}$ [%]	$y_{D,k}$ * [%]	ε_k [%]	$c_{F,k}$ [Cent/MJ]	$c_{P,k}$ [Cent/MJ]	$\dot{C}_{D,k}$ [Cent/s]	Z_K [Cent/s]	f_K [%]	r_K [%]
Compressor	212.46	203.36	9.09	1.54	5.85	95.72	1.36	1.53	12.39	22.61	64.60	12.50
CC	590.23	419.06	171.17	28.94	110.17	71.00	0.76	1.11	130.01	16.15	11.05	46.05
GT	447.95	428.33	19.62	3.32	12.63	95.62	1.24	1.36	24.43	25.84	51.40	9.68
HP2 SH	67.59	64.23	3.36	0.57	2.17	95.02	1.24	1.48	4.19	10.94	72.31	19.35
HP2 Evap	34.47	31.79	2.68	0.45	1.73	92.22	1.24	1.47	3.34	3.87	53.68	18.55
IP2 SH	1.81	1.62	0.19	0.03	0.13	89.24	1.24	1.70	0.24	0.50	67.57	37.10
HP2 Econ	15.39	13.21	2.18	0.37	1.40	85.85	1.24	1.52	2.71	0.95	25.96	22.58
IP2 Evap	7.27	6.82	0.44	0.08	0.29	93.89	1.24	1.62	0.55	1.99	78.35	30.65
IP2 Econ	9.24	7.11	2.13	0.36	1.37	76.90	1.24	1.69	2.66	0.54	16.88	36.29
LP2 Evap	14.76	12.50	2.26	0.38	1.45	84.70	1.24	1.78	2.81	3.89	58.06	43.55
LP2 Econ	0.64	0.53	0.12	0.02	0.08	81.88	1.24	2.37	0.15	0.45	75.00	91.13
Preheater	14.91	11.28	3.63	0.61	2.33	75.67	1.24	2.10	4.52	5.17	53.35	69.35
HP1 SH	15.24	13.91	1.33	0.22	0.85	91.29	0.96	1.29	1.27	3.39	72.75	34.38
HP1 Evap	66.73	61.11	5.63	0.95	3.62	91.57	0.96	1.21	5.40	10.08	65.12	26.04
HP1 Econ	36.42	30.17	6.25	1.06	4.02	82.83	0.96	1.23	6.00	2.08	25.74	28.13
IP1 SH	1.69	1.48	0.20	0.03	0.13	87.85	0.96	1.40	0.20	0.46	69.70	45.83
IP1 Evap	19.93	16.99	2.94	0.50	1.89	85.25	0.96	1.23	2.82	1.80	38.96	28.13
IP1 Econ	4.95	3.71	1.25	0.21	0.80	74.85	0.96	1.35	1.19	0.24	16.78	40.63
P1	2.84	2.15	0.69	0.12	0.44	75.87	1.57	3.03	1.08	2.07	65.71	92.99
Solar field	263.99	142.81	121.18	-	-	54.10	-	0.93	-	132.50	-	-
ST1	50.72	47.00	3.73	0.63	2.40	92.65	1.45	1.72	5.42	7.13	56.81	18.62
ST2	79.91	72.02	7.88	1.33	5.07	90.14	1.45	1.74	11.45	9.22	44.61	20.00
ST3	48.27	43.01	5.26	0.89	3.38	89.11	1.47	1.80	7.71	6.76	46.72	22.45
ST4	74.34	64.89	9.45	1.60	6.08	87.29	1.47	1.81	13.85	8.60	38.31	23.13
P2	0.02	0.01	0	0	0	73.36	1.57	9.82	0.01	0.10	90.91	525.48
P3	1.03	0.75	0.27	0.05	0.18	73.43	1.57	3.37	0.43	0.93	68.38	114.65
P4	2.29	1.70	0.59	0.10	0.38	74.23	1.57	3.15	0.93	1.76	65.43	100.64
P5	0.13	0.09	0.04	0.01	0.03	68.99	1.57	3.54	0.06	0.11	64.71	125.48
Cond	-	-	9.35	1.58	6.02	-	32.29	-	301.89	2.57	0.84	-100
Cooling Tower	-	-	22.7	3.84	14.61	-	34.86	-	791.16	2.74	0.35	-100
Deaerator	8.06	7.25	0.82	0.14	0.53	89.86	1.83	2.23	1.49	1.46	49.49	21.86
mixer 1	0.40	0.38	0.02	0	0.02	94.00	1.35	1.44	0.03	-	-	6.67
mixer 2	4.51	4.36	0.15	0.03	0.10	96.58	1.34	1.39	0.21	-	-	3.73
mixer 3	15.32	12.65	2.67	0.45	1.72	82.55	1.43	1.73	3.83	-	-	20.98
mixer 4	1.27	1.24	0.03	0.01	0.02	97.36	1.45	1.49	0.05	-	-	2.76
mixer 5	0.13	0.10	0.03	0.01	0.02	74.15	1.83	2.46	0.06	-	-	34.43
TOTAL	591.52	436.50	155.37	26.27	100	73.79	0.76	1.68	117.75	286.92	-	-

Table 13. CSP integrated combined cycle power plant with dry cooling results at the component level

Component	$\dot{E}_{F,k}$ [MW]	$\dot{E}_{P,k}$ [MW]	$\dot{E}_{D,k}$ [MW]	$y_{D,k}$ [%]	$y_{D,k}$ * [%]	ε_k [%]	$c_{F,k}$ [Cent/MJ]	$c_{P,k}$ [Cent/MJ]	$\dot{C}_{D,k}$ [Cent/s]	Z_K [Cent/s]	f_K [%]	r_K [%]
Compressor	243.80	233.72	10.09	1.58	6.42	95.86	1.36	1.52	13.68	24.73	64.38	11.76
CC	635.05	454.56	180.49	28.36	114.97	71.58	0.76	1.10	137.08	17.66	11.41	44.74
GT	505.49	483.14	22.35	3.51	14.24	95.58	1.24	1.36	27.72	28.26	50.48	9.68
HP2 SH	67.32	63.87	3.45	0.54	2.19	94.88	1.24	1.47	4.27	10.62	71.32	18.55
HP2 Evap	37.60	34.65	2.95	0.46	1.88	92.15	1.24	1.46	3.66	4.09	52.77	17.74
IP2 SH	1.94	1.73	0.21	0.03	0.13	89.12	1.24	1.69	0.26	0.52	66.67	36.29
HP2 Econ	16.11	13.81	2.30	0.36	1.46	85.74	1.24	1.52	2.85	0.97	25.39	22.58
IP2 Evap	8.26	7.75	0.52	0.08	0.33	93.76	1.24	1.60	0.64	2.15	77.06	29.03
IP2 Econ	9.47	7.27	2.21	0.35	1.41	76.70	1.24	1.69	2.74	0.54	16.46	36.29
LP2 Evap	16.35	13.81	2.54	0.40	1.62	84.46	1.24	1.77	3.15	4.13	56.73	42.74
LP2 Econ	0.67	0.54	0.12	0.02	0.08	81.32	1.24	2.36	0.15	0.45	75.00	90.32
Preheater	14.17	10.62	3.55	0.56	2.26	74.94	1.24	2.02	4.40	3.85	46.67	62.90
HP1 SH	15.24	13.91	1.33	0.21	0.85	91.29	0.95	1.28	1.26	3.34	72.61	34.74
HP1 Evap	66.73	61.11	5.63	0.88	3.58	91.57	0.95	1.20	5.33	9.96	65.14	26.32
HP1 Econ	36.42	30.17	6.25	0.98	3.98	82.83	0.95	1.21	5.92	2.05	25.72	27.37
IP1 SH	1.69	1.48	0.20	0.03	0.13	87.85	0.95	1.38	0.19	0.45	70.31	45.26
IP1 Evap	19.93	16.99	2.94	0.46	1.87	85.25	0.95	1.22	2.78	1.78	39.04	28.42
IP1 Econ	4.95	3.71	1.25	0.20	0.79	74.85	0.95	1.33	1.18	0.23	16.31	40.00
P1	2.84	2.15	0.69	0.11	0.44	75.87	1.54	2.98	1.06	2.05	65.92	93.51
Solar field	263.99	142.81	121.18	-	-	54.10	-	0.92	-	130.81	-	-
ST1	51.57	47.78	3.79	0.60	2.41	92.65	1.44	1.70	5.44	7.11	56.65	18.06
ST2	81.45	73.42	8.03	1.26	5.12	90.14	1.44	1.72	11.53	9.20	44.38	19.44
ST3	49.60	44.20	5.40	0.85	3.44	89.11	1.45	1.78	7.84	6.79	46.41	22.76
ST4	56.12	49.27	6.84	1.08	4.36	87.80	1.45	1.80	9.94	7.20	42.01	24.14
P2	0.02	0.01	0.00	0.00	0.00	73.36	1.54	9.58	0.01	0.10	90.91	522.08
P3	1.05	0.77	0.28	0.04	0.18	73.43	1.54	3.31	0.43	0.93	68.38	114.94
P4	2.33	1.73	0.60	0.09	0.38	74.23	1.54	3.09	0.92	1.76	65.67	100.65
P5	0.13	0.09	0.04	0.01	0.02	69.75	1.54	3.32	0.06	0.10	62.50	115.58
AC Cond	52.42	-	22.40	3.52	14.27	1.91	1.47	-	32.91	21.48	39.49	-
Deaerator	8.25	7.42	0.83	0.13	0.53	89.89	1.80	2.21	1.50	1.49	49.83	22.78
mixer 1	0.44	0.41	0.03	0.00	0.02	94.13	1.33	1.41	0.03	-	-	6.02
mixer 2	4.78	4.62	0.16	0.03	0.10	96.61	1.32	1.37	0.21	-	-	3.79
mixer 3	13.17	10.90	2.26	0.36	1.44	82.81	1.42	1.71	3.21	-	-	20.42
mixer 4	1.31	1.28	0.03	0.01	0.02	97.36	1.44	1.48	0.05	-	-	2.78
mixer 5	0.16	0.12	0.04	0.01	0.03	74.11	1.80	2.43	0.08	-	-	35.00
TOTAL	636.44	437.12	156.99	24.67	100	68.68	0.76	1.80	118.97	304.82	-	-